Journal of Medicinal Chemistry

Article

Novel Bioactive Hybrid Compounds Dual Targeting Estrogen Receptor and Histone Deacetylase for Treatment of Breast Cancer

Chu Tang, Changhao Li, Silong Zhang, Zhiye Hu, Jun Wu, Chune Dong, Jian Huang, and Hai-Bing Zhou

J. Med. Chem., **Just Accepted Manuscript** • Publication Date (Web): 20 May 2015

Novel Bioactive Hybrid Compounds Dual Targeting Estrogen Receptor and Histone Deacetylase for Treatment of Breast Cancer

Chu Tang,[a‡] Changhao Li,[b‡] Silong Zhang,[a] Zhiye Hu,[a] Jun Wu,[b] Chune Dong,[a]* Jian Huang,[b]* and Hai-Bing Zhou[a]*

[a] State Key Laboratory of Virology;
Key Laboratory of Combinatorial Biosynthesis and Drug Discovery (Wuhan University), Ministry of Education;
Wuhan University School of Pharmaceutical Sciences, Wuhan, 430071, China;
[b] College of Life Sciences, Wuhan University, Wuhan, 430072, China
[‡] These two authors contributed equally to this work

ABSTRACT

A strategy to develop chemotherapeutic agents by combining several active groups into a single molecule as a conjugate that can modulate multiple cellular pathways may produce compounds having higher efficacy compared to single-target drugs. In this paper, we describe the synthesis and evaluation of an array of dual-acting ER and histone deacetylase inhibitors. These novel hybrid compounds combine an indirect antagonism structure motif of ER (OBHS, oxabicycloheptene sulfonate) with the HDAC inhibitor suberoylanilide hydroxamic acid (SAHA). These OBHS-HDACi conjugates exhibited good ER binding affinity and excellent ERα antagonistic activity, and they also exhibited potent inhibitory activities against HDACs. Compared with the approved drug tamoxifen, these conjugates exhibited higher antitumor potency in ERα-positive breast cancer cells (MCF-7). Moreover, these conjugates not only showed selective anticancer activity that was more potent against MCF-7 cells than DU 145 (prostate cancer), but they had no toxicity towards normal cells.

INTRODUCTION

Breast cancer is the most common cancer among women, and approximately 230,000 breast cancer cases are reported per year in the United States, of which approximately 13,000 are diagnosed in women aged less than 40 years.[1] The estrogen receptor (ER), which is a ligand-regulated transcription factor that regulates many physiological and pathological processes, plays a predominant role in breast cancer growth.[2, 3] Therefore, ER is regarded as important pharmaceutical target for the treatment of breast cancer, and development of ER ligands has emerged as active study field in the fight against breast cancer. Many of these ligands have been developed into hormone agents, which often have mixed agonist-antagonist and tissue-selective activities. Some of these agents have been termed selective estrogen receptor modulators (SERMs),[4, 5] which are the most recently approved class of first line drugs for the treatment of breast cancer. Tamoxifen is the first clinically used SERM for the prevention and treatment of breast cancer.[6, 7]

Although current SERMs have clear advantages in the treatment of hormone-responsive breast cancer, they retain some disadvantages. For instance, tamoxifen therapy is ineffective for ER(-) and triple-negative breast (TNB) cancers, and roughly half of ER(+) tumors are insensitive or gain resistance, losing their response to continued tamoxifen therapy.[8-10] Thus, much effort has been undertaken to develop an "ideal SERM", one that is more effective or one towards which resistance does not develop.[11] One strategy to develop such SERMs involves combining two bioactive drugs into a single molecule, forming a conjugate that can interact with two relevant components of breast cancer process and thus might possess enhanced therapeutic activity.[12]

In taking this approach, the attachment of anti-tumor agents to the functional groups of the ER ligands, estradiol or tamoxifen, has been used to form conjugates that exhibited enhanced pharmacological properties. For example, conjugates have been made with an intercalating agent (E_2-ellipticine conjugate **1**, Figure 1),[13] an alkylating agent (E_2-chlorambucil conjugate **2**, Figure 1),[14] or an antimitotic (tamoxifen-doxorubicin conjugate **3**, Figure 1).[15] Although these conjugates have very

potent anti-cancer activity, because of their extremely low ER binding affinity, they lack the cell-type or target-tissue selectivity, which severely limits their clinical utility. So far, the estrogen receptor targeting agents used to form these types of conjugates have mostly been estradiol or tamoxifen; other ER ligands have rarely been chosen.

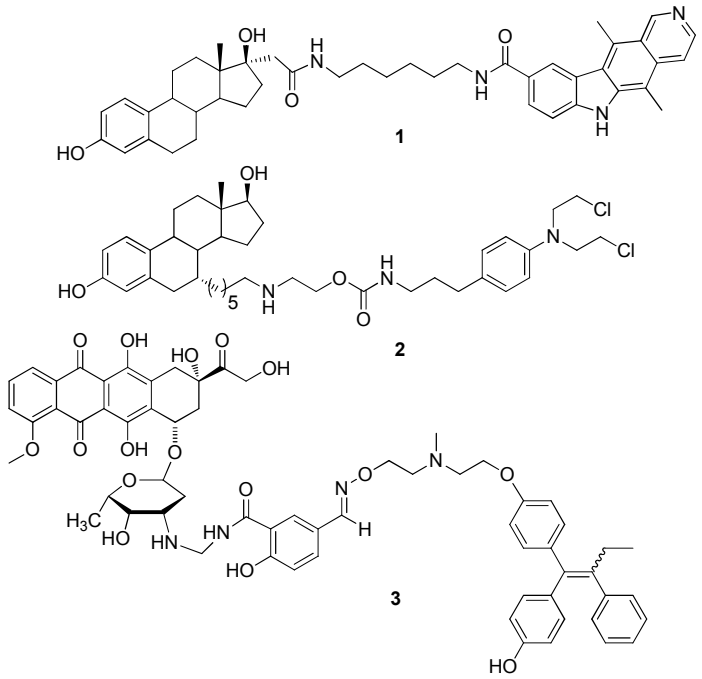

Figure 1. (**1**) E_2-ellipticine conjugate; (**2**) E_2-chlorambucil conjugate; (**3**) tamoxifen-doxorubicin conjugate.

As part of our ongoing interest in the development of ER ligands having therapeutic efficacy on breast cancer,[16-18] we have focused on the preparation and evaluation of novel ER ligands having a more three-dimensional character. Among them, *exo*-5,6-bis-(4-hydroxyphenyl)-7-oxabicyclo[2.2.1]hept-5-ene-2-sulfonic acid phenyl ester (OBHS), was one of the best compounds, exhibiting modest ER subtype selectivity, with relative binding affinity (RBA) values of 9.3% and 1.7% (data from reference 16) for ERα and ERβ, respectively (RBA[estradiol] = 100%), and was a partial antagonist on both ERs (Figure 2).[16] Although OBHS bears no structural resemblance to other estrogen antagonists, analysis of the X-ray crystal structure of the complex of ERα-LBD with OBHS indicates that its partial antagonist character was achieved by indirectly modulating the critical switch helix in the ER ligand binding domain, helix 12, by interactions with helix 11. The crystal structure also

shows that the phenyl sulfonate group of OBHS plays an important role in producing the partial antagonist activity of OBHS: The sulfonate phenol binds between helices 8 and 11, and by making a strong steric clash with helix 11, it displaces His524 outward and repositions helix 11 so that it indirectly modulates the orientation of the helix 12, eventually destroying the surface-bound coactivator binding site. Furthermore, in contrast to the mechanism action of tamoxifen that directly relocates helix 12 through its interaction with the bulky and basic side chain, OBHS has two 4-hydroxyphenyl substituents, one which of which mimics the hydroxyphenyl of estradiol, engaging in strong hydrogen bond with E353; the other one points in the E_2 11β direction, but it is not long enough to interact directly with helix 12. Therefore, this second phenol group can be replaced or modified with a range of functional group to enhance the antagonist properties of these oxabicyclo[2.2.1]heptene core ligands.[19]

With regard to the design of our conjugates, it is notable that estrogen signaling requires the displacement of certain proteins, for example, HDACs, from corepressor complexes, and the recruitment of coactivator proteins to transcription complexes containing liganded ER.[20] Solid evidence supports the direct interaction of HDACs with corepressor proteins and ER in silenced nuclear transcription complexes in the cell nucleus, for example, the interaction of HDAC1 with the activation function 2 (AF2) and DNA binding domain (DBD) of ERα.[21] In ER(+) cells, knockdown of HDAC1 and HDAC inhibition by either trichostatin A (TSA), valproic acid (VPA), or butyric acid, can decrease ERα levels.[22-25] Thus, because the combination of SERM activity with HDAC inhibitor therapy requires both drug components to be in close proximity in the cell nucleus, the concept of an HDAC inhibitor combined with a SERM in a single molecule hybrid or conjugate is thus proposed.[26] A recent phase II clinical study also revealed that the use of a combination of the HDAC inhibitor, SAHA, and the SERM, tamoxifen, as separate agents, could increase the efficacy of tamoxifen.[27]

Thus, to address the need for more effective drugs for breast cancer, we chose the clinically effective HDACi (SAHA) as the second component of our conjugate, hypothesizing that the incorporation of SAHA into unique ER ligands might produce

new bifunctional hybrid agents having improved efficacy and selectivity while retaining high affinity for ER. In light of our interest in ER ligands, we expanded the diversity of OBHS by equipping this ligand in two ways with the histone deacetylase inhibitor (HDACi) SAHA so as to confer selective anti-tumor activity against breast cancers (Figure 2).

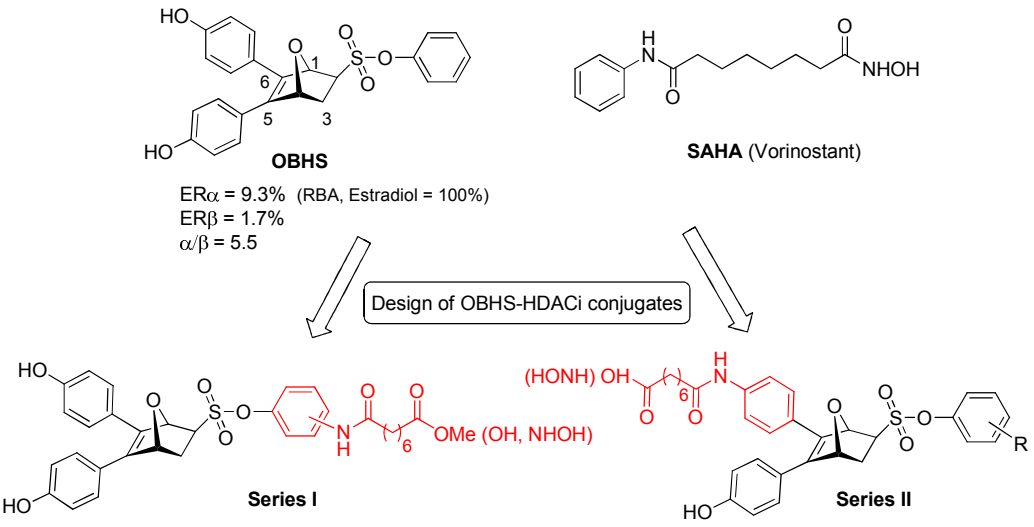

Figure 2. Design of dual-acting OBHS-HDACi conjugates.

Herein, we describe the design and biological evaluation of novel OBHS-HDACi conjugates, which can be prepared conveniently by a Diels-Alder reaction of a furan with an appropriate dienophile. The OBHS-SAHA conjugates of this design not only have three-dimensional topology, but also have second pharmacologically HDACi unit. Thus they expand our exploration of novel estrogen receptor ligand. For comparison, the ester and carboxylic acid analogues (by replacing the hydroxamic acid (-CONHOH) group with (-COOH) or methyl ester (-COOMe)) were also prepared and evaluated for their ER binding affinity, estrogen responsive element-driven transcriptional activity, HDAC inhibition activity, cell antiproliferative activity and selectivity *etc*.

RESULTS AND DISCUSSION

Chemical Synthesis. All designed OBHS-HDACi conjugates were synthesized by a Diels-Alder reaction of 3,4-bis(4-hydroxyphenyl)furan **4** (cf. Scheme 3A) or furan derivative **12** with various dienophiles. The 3,4-bis(4-hydroxyphenyl)furan **4** was

prepared according to our previously developed methodology.[16] 8-(4-(4-(4-Hydroxyphenyl)furan-3-yl)-phenylamino)-8-oxooctanoic acid **12** was the key intermediate in the synthesis of OBHS-HDACi conjugates, and it was synthesized by the general route depicted in Scheme 1. Treatment of 4-methoxyacetophenone **5** with *N*-bromosuccinimide in the presence of *p*-toluenesulfonic acid provided α-bromo-4-methoxyacetophenone **6** in 95% yield. **8** was formed by reaction of **6** with 4-aminophenylacetic acid **7** in the presence of triethylamine in acetonitrile, followed by an Aldol reaction to give **9**, which was demethylated with BBr_3 to afford butenolide **10**. Diisobutylaluminum hydride reduction of **10** at -78 °C gave, after acidic workup with 4% H_2SO_4, the furan **11**, which was allowed to react with suberic anhydride to obtain the key intermediate **12**.

The synthesis of various vinyl sulfonates **16a-b**, **19a-r** was accomplished by the reaction of 2-chloroethanesulfonyl chloride with substituted phenols under basic reaction conditions, as shown in Scheme 2. Vinyl sulfonates **16a-b** could be synthesized by a three-step procedure from commercially available suberic acid via suberic anhydride. First, suberic anhydride **14** was prepared from a mixture of suberic acid **13** with acetic anhydride.[28] Then, suberic anhydride **14** was condensed with the corresponding aminophenol to generate compounds **15a-b**, which were subsequently reacted with 2-chloroethanesulfonyl chloride to yield the vinyl sulfonates **16a-b** (Scheme 2A). The various commercially available substituted phenols were reacted with 2-chloroethanesulfonyl chloride to yield the corresponding vinyl sulfonates **19a-r** (Scheme 2B). The synthesis of OBHS-HDACi conjugates was effectively accomplished by a Diels-Alder reaction of furan **4** or **12** with various vinyl sulfonates (Scheme 3); the results were summarized in Table 1.

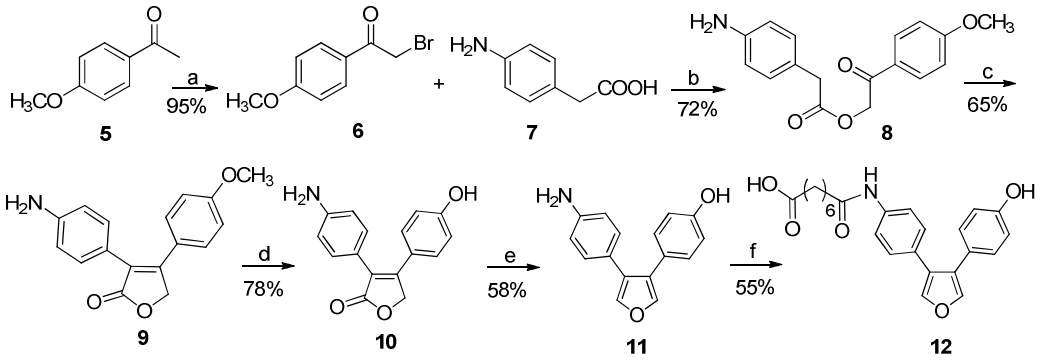

Scheme 1. Synthesis of furan derivative **12**. Reagents and conditions: (a) NBS (1.2 equiv.), *p*-TsOH (0.2 equiv.), $CHCl_3$, rt, 12h; (b) Et_3N, CH_3CN, rt, 12h; (c) NaH, DMSO, rt, 3h; (d) BBr_3, CH_2Cl_2, -20 °C, 12h; (e) DIBAL-H, THF, -78 °C, 8h; (f) suberic anhydride , THF, rt, 2h.

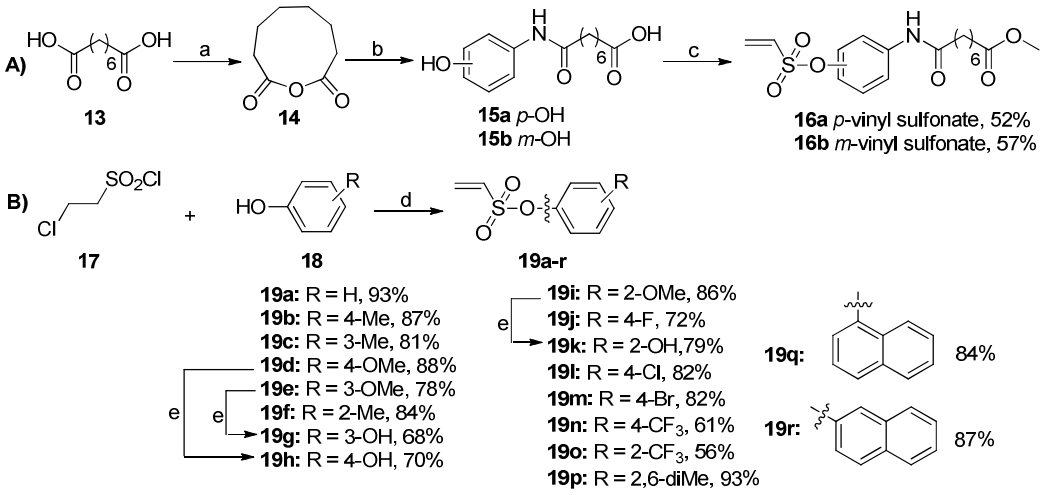

Scheme 2. Synthesis of dienophiles **16a-b**, **19a-r**. Reagents and conditions: (a) acetic anhydride, 150 °C, 1h; (b) 4-aminophenol or 3-aminophenol, THF, rt, 1h; (c) (i) 2-chloroethanesulfonyl chloride, Et_3N, THF, 0 °C, 12h; (ii) MeOH, rt, 12h (d) Et_3N, CH_2Cl_2, 0 °C, 12h; (e) BBr_3, CH_2Cl_2, -20 °C, 12h.

The Diels-Alder reaction of vinyl sulfonates with furans (**4** or **12**) went very smoothly, and the yields of the products were generally good. Also, it is noteworthy that high stereoselectivity was observed in the reaction of furans with dienophiles; as we described previously,[16] the *exo* products predominated in the Diels-Alder reaction. The compound **4** was a symmetrical furan; therefore, the Diels-Alder products **20a-b**, **21a-b** and **22** were studied single isomers, and among them, **21a** showed the highest binding affinity (see below). The Diels-Alder reactions of vinyl sulfonates with the

unsymmetrical furan **12** produces the conjugates **23a-r**, **24a-i**, which were studied as a mixture of regioisomers that, despite our best efforts, could not be separated. The low affinity of these conjugates compared to OBHS make this less of an issue. As mentioned above and reported previously, the isolated products are the *exo* diastereomers; they are also racemates.

During our work on OBHS-core ER ligands, we found that the disposition and size of the substituents on phenyl ring of the OBHS sulfonate moiety were important determinants of the binding affinity and selectivity of these compounds. First, we introduced the SAHA group on the phenyl sulfonate unit (Scheme 3A, Series I). Reaction of **4** with **16a-b** afforded the ester **20a-b**, and hydrolysis in basic medium (NaOH, 2 N) gave carboxylic acid derivatives **21a-b**. Treatment of **21a** with KOH/NH_2OH in THF after activation of the carboxylate afforded the final hydroxamic acid **22**.[28, 29] However, we found the carboxylic acid derivative **21a** had higher ER binding affinity than ester **20a** and hydroxamate **22** in series I. Although compounds having carboxylic acid have rarely been studied, Jaouen, *et al*. prepared a series of tamoxifen-SAHA conjugates in which the carboxylic acid derivative also had higher ERα affinity compared to hydroxamic acid analogue, and biological assay results indicated that the carboxylic acid derivative was a more potent inhibitor of MCF-7 cells.[30] Therefore, we wondered whether the replacement of the hydroxamate unit with the carboxylic acid might also elevate the binding affinity of our OBHS conjugates. Thus, when the SAHA group was appended onto one of phenol rings on C-5 or C-6 of OBHS (Scheme 3B, Series II), additional SAR investigations were also focused on the carboxylic acid derivatives **23a-r** as well as on selected hydroxamate analogs **24a-i** that were derived from the carboxylic acid derivatives having better binding affinities. This hypothesis was verified by the fact that the **23a-c**, **23f**, **23i-j**, **23m**, **23q-r** had high ER binding affinity in series II; however, when **23a-c**, **23f**, **23i-j**, **23m**, **23q-r** were transformed into the hydroxamate **24a-i** with NH_2OH after activation (Scheme 3, Figure 4), ER binding affinity was significantly decreased (see below).

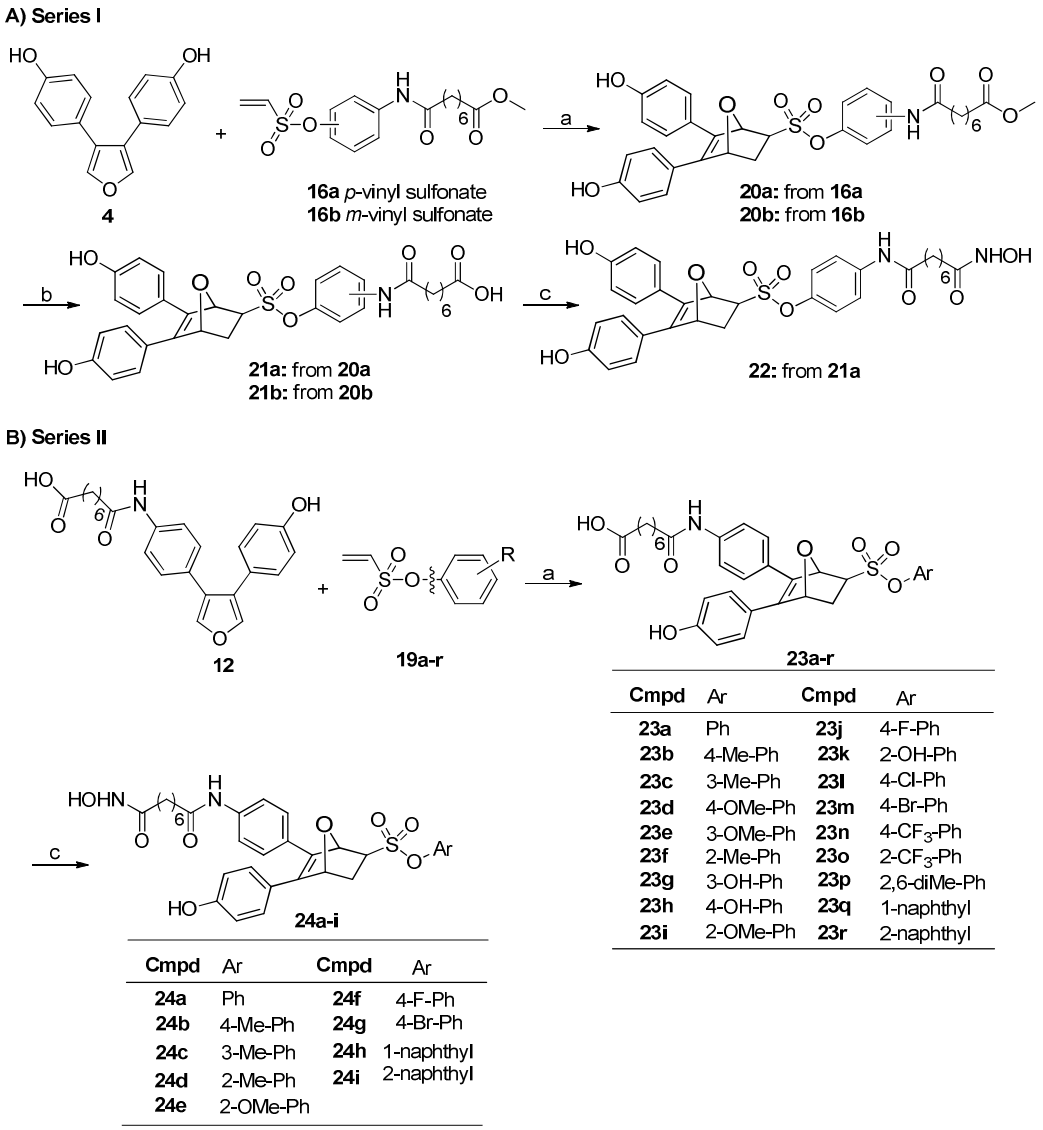

Cmpd	Ar	Cmpd	Ar
23a	Ph	**23j**	4-F-Ph
23b	4-Me-Ph	**23k**	2-OH-Ph
23c	3-Me-Ph	**23l**	4-Cl-Ph
23d	4-OMe-Ph	**23m**	4-Br-Ph
23e	3-OMe-Ph	**23n**	4-CF_3-Ph
23f	2-Me-Ph	**23o**	2-CF_3-Ph
23g	3-OH-Ph	**23p**	2,6-diMe-Ph
23h	4-OH-Ph	**23q**	1-naphthyl
23i	2-OMe-Ph	**23r**	2-naphthyl

Cmpd	Ar	Cmpd	Ar
24a	Ph	**24f**	4-F-Ph
24b	4-Me-Ph	**24g**	4-Br-Ph
24c	3-Me-Ph	**24h**	1-naphthyl
24d	2-Me-Ph	**24i**	2-naphthyl
24e	2-OMe-Ph		

Scheme 3. Synthesis of OBHS-HDACi conjugates **20a-b**, **21a-b**, **22**, **23a-r** and **24a-i**. Reagents and conditions: (a) neat, 90 °C, 12h; (b) KOH, MeOH, rt, 3h; (c) $ClCO_2Et$, KOH, THF, 0 °C, 15 min and then $NH_2OH{\cdot}HCl$, KOH, MeOH, rt, 1h.

Table 1. Diels-Alder Reaction of Furans **4**, **12** and Dienophiles **16a-b** and **19a-r**

Entry	Furan	Dienophile		Conv.[a] (%)	Product Yield[b]	
1	**4**	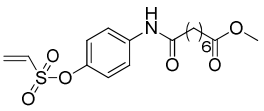	**16a**	98	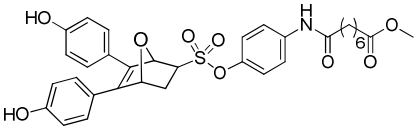	**20a** (91%)
2		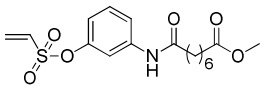	**16b**	97	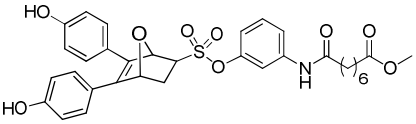	**20b** (89%)
3		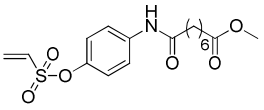	**16a**	96	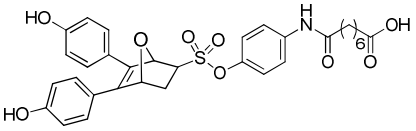	**21a** (86%)
4		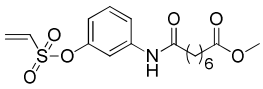	**16b**	96	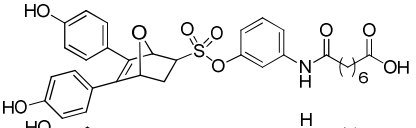	**21b** (87%)
5		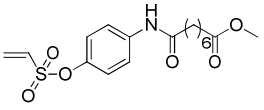	**16a**	84	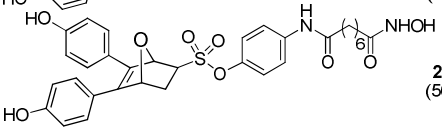	**22** (56%)
6	**12**	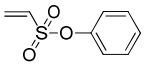	**19a**	99	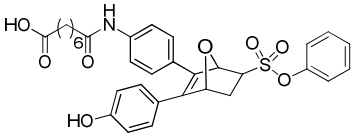	**23a** (95%)
7		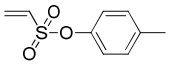	**19b**	98	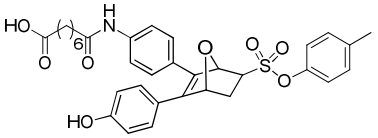	**23b** (94%)
8		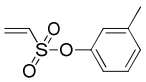	**19c**	99	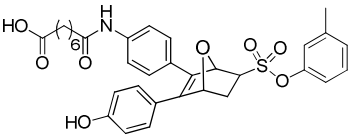	**23c** (92%)
9		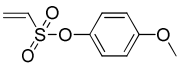	**19d**	99	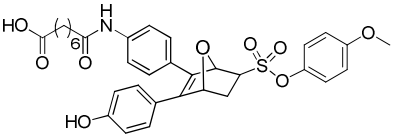	**23d** (92%)
10		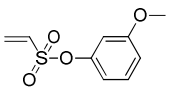	**19e**	98	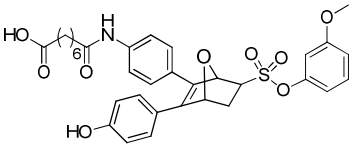	**23e** (89%)

Table 1. Continued

Entry	Furan	Dienophile		Conv.[a] (%)	Product Yield[b]
11	**12**	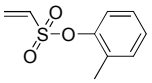	**19f**	95	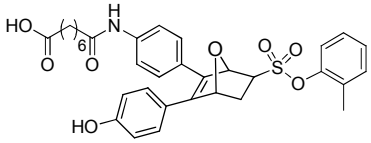 **23f** (92%)
12		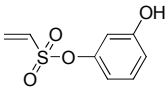	**19g**	85	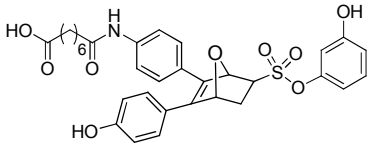 **23g** (76%)
13		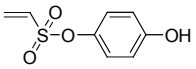	**19h**	88	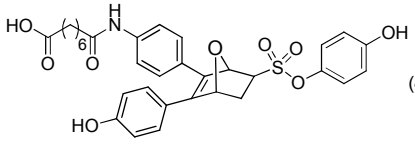 **23h** (83%)
14		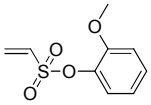	**19i**	99	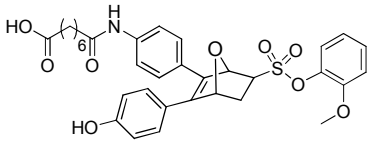 **23i** (96%)
15		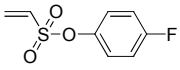	**19j**	82	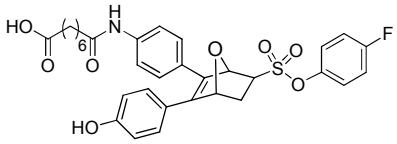 **23j** (78%)
16		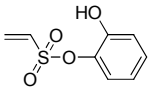	**19k**	87	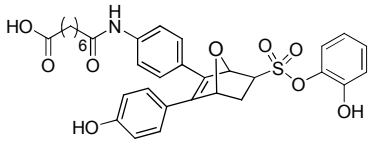 **23k** (81%)
17		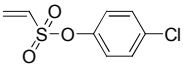	**19l**	80	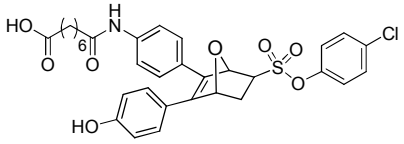 **23l** (74%)
18		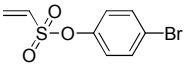	**19m**	78	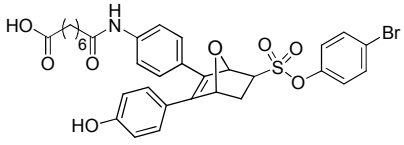 **23m** (72%)
19		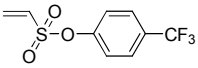	**19n**	88	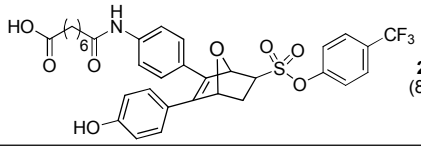 **23n** (82%)

Table 1. Continued

Entry	Furan	Dienophile		Conv.[a] (%)	Product Yield[b]
20	**12**	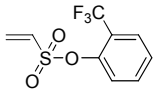	**19o**	87	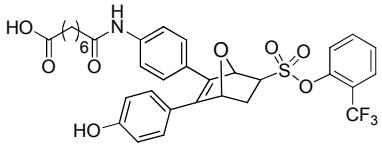 **23o** (80%)
21		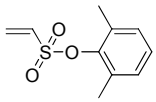	**19p**	100	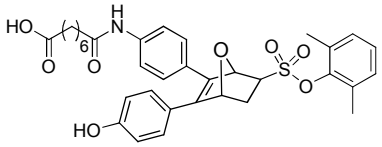 **23p** (93%)
22		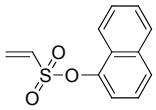	**19q**	98	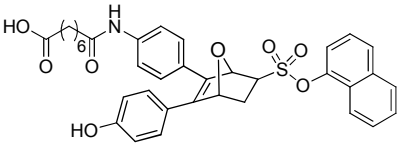 **23q** (90%)
23		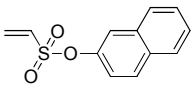	**19r**	100	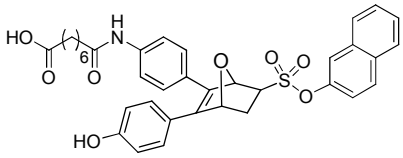 **23r** (94%)
24		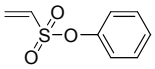	**19a**	93	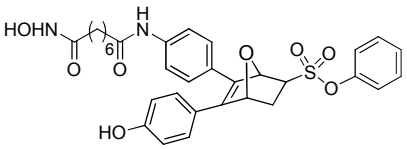 **24a** (76%)
25		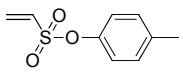	**19b**	96	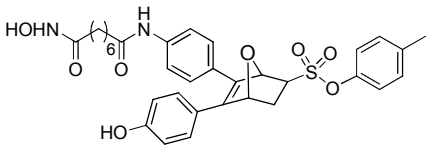 **24b** (83%)
26		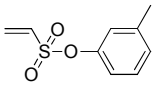	**19c**	95	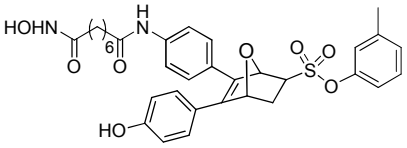 **24c** (79%)
27		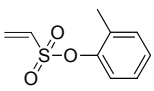	**19f**	88	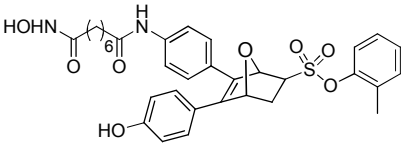 **24d** (76%)

Table 1. Continued

Entry	Furan	Dienophile		Conv.[a] (%)	Product Yield[b]	
28	**12**	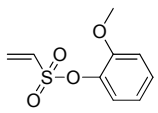	**19i**	90	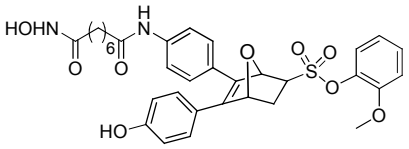	**24e** (87%)
29		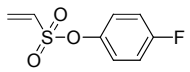	**19j**	81	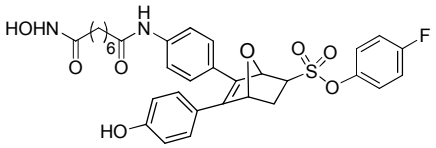	**24f** (73%)
30		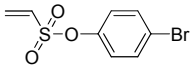	**19m**	78	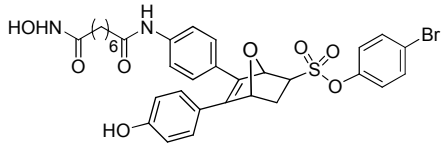	**24g** (70%)
31		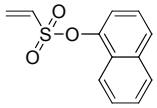	**19q**	92	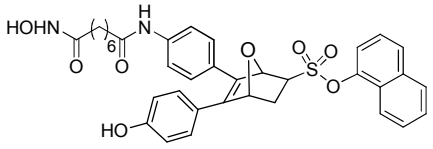	**24h** (88%)
32		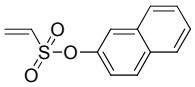	**19r**	96	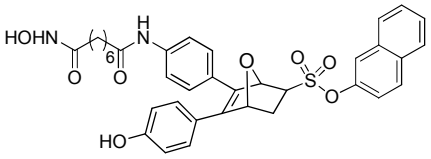	**24i** (85%)

[a]The conversion was calculated accounting for the recovered furan **4** or **12**. [b]Isolated yield by column chromatography purification based on furan **4** or **12**.

ER ligands-HDACi conjugates Exhibit Binding Affinity. The binding affinities of the OBHS-HDACi conjugates for both ERα and ERβ were determined by a competitive fluorometric receptor-binding assay and are summarized in Table 2; the K_i values of the OBHS-HDACi conjugates are also summarized in Table 2.[31] These affinities are presented as relative binding affinity (RBA) values, where estradiol has an affinity of 100%.

As a global observation, it is noteworthy that the position of suberic acid or SAHA group in the phenyl ring of OBHS has very significant effects on the binding affinity of conjugates. In general, the series I of **20a-b**, **21a-b** that possessed the suberic acid group in the phenyl sulfonate moiety demonstrate better binding affinity for ERα than the series II (the suberic acid group was attached to a phenol ring of OBHS). The

compound that has the highest binding affinity for ERα and ER subtype selectivity of all of conjugates is **21a**, a compound that possesses a *para*-suberic acid group on the phenyl sulfonate unit. The RBA values of this compound are 12.4 and 0.44 for ERα and ERβ, respectively, and it has an ERα/ERβ selectivity as high as 28 (Table 2, entry 3). Compared to the parent compound OBHS (RBA values were 14.4 for ERα, 6.93 for ERβ, α/β was 2.08, measured on a sample newly synthesized for this study), the conjugate **21a** still retained high binding affinity for ERα, and had higher selectivity (Table 2, entries 3 vs 33). However, compounds **20a** and **22** (Table 2, entries 3 vs 2 and 5), which replaced carboxylic acid of **21a** with a methyl ester and an hydroxamic acid, respectively, both show lower binding affinity for ERα and reduced subtype selectivity. We are also aware of the substitutional effect that the position of the suberic acid on the phenyl sulfonate unit has on binding affinity for ERα. Compound **21b**, which possesses a *meta*-suberic acid group instead of *para*-suberic acid group as in the series I, shows lower binding affinity for ERα than **21a** (Table 2, entries 3 vs 4).

As is well-known, the presence of a phenolic group in ER ligands is crucial to their binding affinity. OBHS has two phenolic groups, one of which mimics the steroidal "A ring" present in nature estrogens,[32] engaging in strong hydrogen bonds with residues Glu 353 and Arg 394 and a structured water molecule in ERα. The second phenolic group in OBHS makes a distinct hydrogen bond with residue Thr 347. Deletion of the second phenolic OH greatly reduces binding affinity for ERα. Indeed, all of the series II compounds have decreased binding affinity for ERα; however, most of the conjugates exhibit moderate binding affinity for ERβ (Table 2, entries 6-24), and the disposition and the size of substituent on the phenyl sulfonate also prove to be important factors in determining binding affinity in this series.

In the case of **23a**, a compound without a substituent on the phenyl sulfonate, it shows poor binding affinity for ERβ, with an RBA value not exceeding 1. However, introduction of a methyl group (compounds **23b-c**, and **23f**, Table 2, entries 7-8, and 11) resulted in an obvious increase in binding affinity for ERβ, with RBA values ranging from 3.5 to 5.0, with **23c** showing a 10-fold affinity increase for ERβ

compared to **23a**. The position of methyl group, however, has little effect on binding affinity for both ERs. When the methyl group was replaced with methoxyl group (analogues **23d**, **23e**, and **23i**), a progressive decrease of RBA values was observed (Table 2, **23b** vs **23d**; **23c** vs **23e**; **23f** vs **23i**). The *para*-methoxy-substituted compound (**23d**) showed lower binding affinities, but the *ortho* analogue **23i** showed a slight decrease in affinity for both ERs, while the *meta*-methoxyl analogue **23e** showed a significant drop in binding affinity for ERα, but still had good binding affinity for ERβ (Table 2, entry 10).

Some interesting things were also observed with hydroxyl analogues **23g**, **23h**, and **23k**. The position of the hydroxy has a remarkable effect on ERβ affinity: The *para*-hydroxyl compound **23h** is superior to the other two (Table 2, entries 13 vs 12; entries 13 vs 16) and shows a 16-fold increase over **23a** (Table 2, entries 13 vs 6). In fact, compound **23h** has the highest ERβ affinity of all conjugates tested, yet has modest selectivity between ERα and ERβ.

Comparisons of the ERα and ERβ binding affinity of **23b**, **23d**, and **23h** indicates that the substituent at the 4-position of the phenyl sulfonate moiety has a significant effect on the binding affinity, and halogens substitutions were also evaluated. This series (**23j**, **23l**, and **23m**) showed to an increase in the affinity for ERβ, with RBA values ranging from 1 to 6, and the fluoro and bromo compounds seem to be superior to the chloro compound (Table 2, entries 15 vs 17; entries 18 vs 17), whereas the electron-withdrawing trifluoromethyl substituent (**23n**) noticeably decreased ligand binding affinity.

A summary of RBA values of the alternate substituents at 4-position of the phenyl sulfonate moiety is presented in Figure 3. These results illustrate that hydroxyl and halogen substituents have high binding affinity and favor ERβ. Addition of a second methyl, as in the 2,6-dimethyl conjugate **23p**, was found to have about 3000-fold lower affinity for ERα than the 2-methyl analogue **23f** (Table 2, entries 11 vs 21), most likely because of unfavorable steric interactions with the pocket. Other changes to substitutions, such as replacing the phenyl with a naphthyl group, as in compound **23q** and **23r**, which contained a bulkier substituent than **23p**, results in similar

binding affinities as those of the methyl analogues for both ERs. Compound **23q** and **23r** have about 6- to 12-fold higher affinity than **23a** in favor of ERβ. However, when conjugates **23a-c**, **23f**, **23i-j**, **23m** and **23q-r**, which had high binding affinities, were transformed into the corresponding hydroxamates **24a-i**, all of the hydroxamate conjugates showed poor binding affinity for both ERs, except **24i**, which displays *ca* half of RBAs of that of parent compound **23r** for ERα and ERβ, respectively (Figure 4). This result also confirmed that the carboxylic acid compound was superior to the hydroxamate compound in terms of ER binding (Table 2, entries 4 vs 5).

Table 2. Relative Binding Affinity (RBA) of OBHS-HDACi Conjugates for ERα and ERβ[α]

Entry	Compound		RBA[a] (%) ERα	RBA[a] (%) ERβ	α/β ratio	K_i[b] (nM) ERα	K_i[b] (nM) ERβ	α/β ratio
1	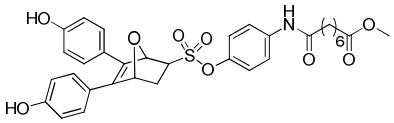	**20a**	5.18 ± 0.37	0.45 ± 0.14	11.51	59.86	755.56	12.62
2	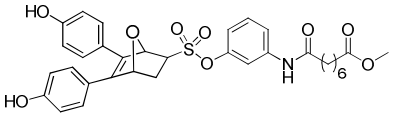	**20b**	4.36 ± 0.29	0.24 ± 0.00	18.17	71.10	1416.67	19.92
3	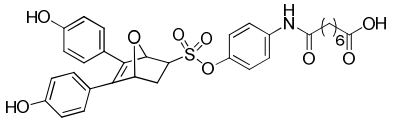	**21a**	12.4 ± 0.98	0.44 ± 0.04	28.18	25.00	772.73	30.91
4	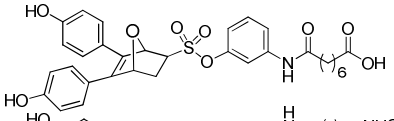	**21b**	5.48 ± 0.64	0.54 ± 0.12	10.14	56.57	629.63	11.13
5	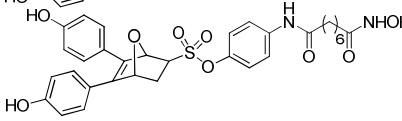	**22**	2.10 ± 0.06	2.68 ± 0.06	0.78	147.62	126.87	0.86
6	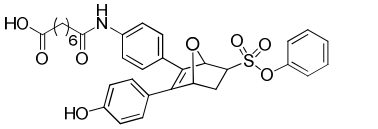	**23a**	2.77 ± 0.35	0.52 ± 0.05	5.33	111.91	653.85	5.84
7	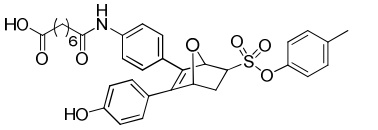	**23b**	1.70 ± 0.29	3.55 ± 0.31	0.49	182.35	87.32	0.48
8	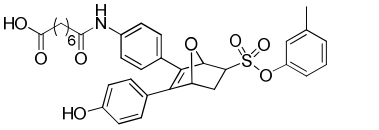	**23c**	3.85 ± 0.56	5.02 ± 0.49	0.77	80.52	67.73	0.84
9	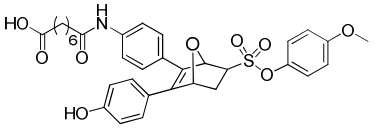	**23d**	0.13 ± 0.00	0.55 ± 0.03	0.24	2384.62	618.18	0.26
10	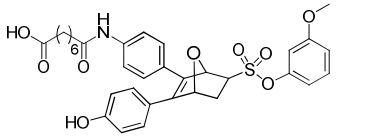	**23e**	0.07 ± 0.14	4.17 ± 1.56	0.02	4428.57	81.53	0.02

Table 2. Continued

Entry	Compound		RBA[a] (%) ERα	RBA[a] (%) ERβ	α/β ratio	K_i[b] (nM) ERα	K_i[b] (nM) ERβ	α/β ratio
11	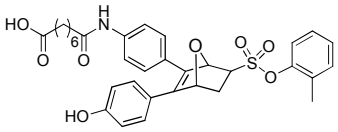	**23f**	2.98 ± 0.75	3.70 ± 0.21	0.81	104.02	91.89	0.88
12	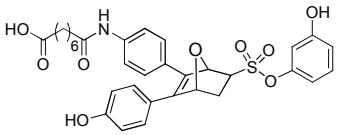	**23g**	3.81 ± 0.04	3.35 ± 0.24	1.14	81.36	101.49	1.25
13	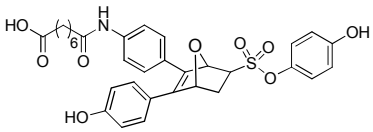	**23h**	2.33 ± 0.27	8.71 ± 1.02	0.27	133.05	39.04	0.29
14	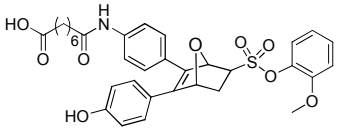	**23i**	1.95 ± 0.30	3.57 ± 0.16	0.55	158.97	95.24	0.60
15	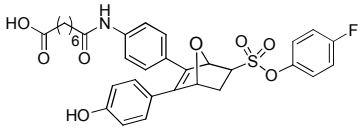	**23j**	3.36 ± 0.49	6.83 ± 0.37	0.49	92.26	49.78	0.54
16	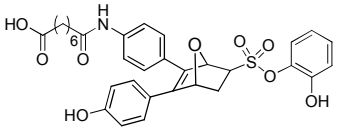	**23k**	0.26 ± 0.05	2.80 ± 0.08	0.09	1192.30	121.43	0.10
17	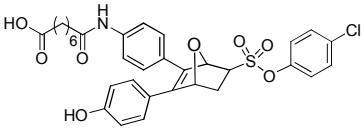	**23l**	2.46 ± 0.24	1.70 ± 0.05	1.45	126.02	200.01	1.59
18	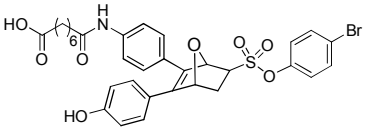	**23m**	2.47 ± 0.03	5.62 ± 0.39	0.40	125.51	60.50	0.48
19	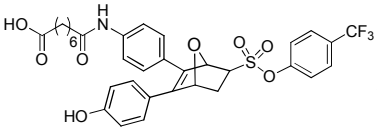	**23n**	0.18 ± 0.03	1.33 ± 0.16	0.14	1722.22	255.64	0.15

Table 2. Continued

Entry	Compound		RBA[a] (%) ERα	RBA[a] (%) ERβ	α/β ratio	K_i[b] (nM) ERα	K_i[b] (nM) ERβ	α/β ratio
20	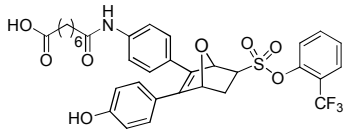	**23o**	0.08 ± 0.01	0.71 ± 0.10	0.11	3875.00	478.87	0.12
21	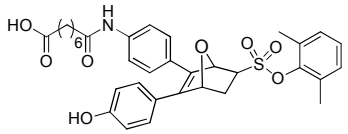	**23p**	0.01 ± 0.00	0.35 ± 0.14	0.029	> 5000	971.43	< 0.19
22	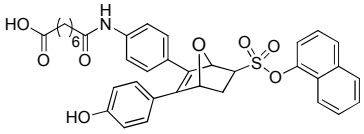	**23q**	2.55 ± 0.56	3.35 ± 0.34	0.76	121.57	101.49	0.83
23	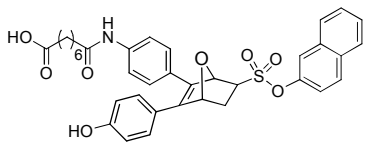	**23r**	1.83 ± 0.16	6.11 ± 0.37	0.30	169.40	55.65	0.33
24	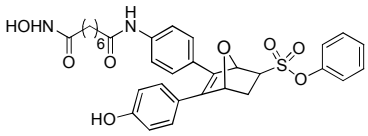	**24a**	0.01 ± 0.00	0.11 ± 0.01	0.09	> 5000	3090.90	< 0.62
25	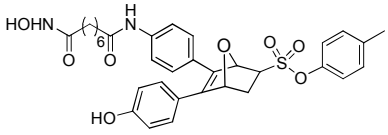	**24b**	0.04 ± 0.01	0.04 ± 0.00	1.00	> 5000	> 5000	1.00
26	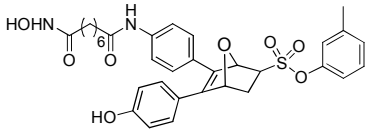	**24c**	0.07 ± 0.04	< 0.01	> 7	4428.57	> 5000	> 1.29
27	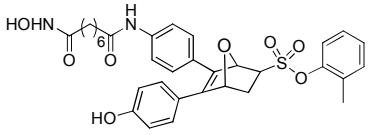	**24d**	0.04 ± 0.00	0.16 ± 0.04	0.25	> 5000	2125.00	< 0.43

Table 2. Continued

Entry	Compound		RBA[a] (%) ERα	RBA[a] (%) ERβ	α/β ratio	K_i[b] (nM) ERα	K_i[b] (nM) ERβ	α/β ratio
28	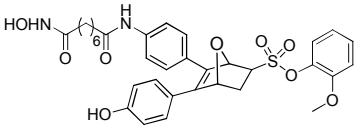	**24e**	0.04 ± 0.01	0.12 ± 0.00	0.33	> 5000	2833.33	< 0.57
29	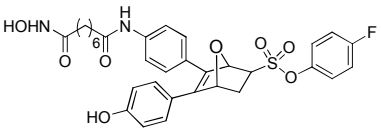	**24f**	0.01 ± 0.00	0.10 ± 0.01	0.10	> 5000	3400.00	< 0.68
30	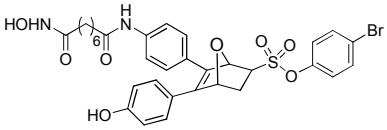	**24g**	0.03 ± 0.00	0.14 ± 0.01	0.21	> 5000	2428.57	< 0.49
31	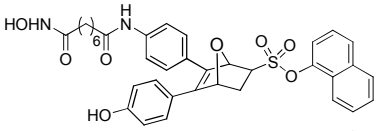	**24h**	0.05 ± 0.01	0.42 ± 0.02	0.12	> 5000	809.52	< 0.16
32	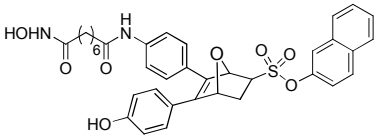	**24i**	1.01 ± 0.16	3.32 ± 0.38	0.30	306.93	102.41	0.33
33	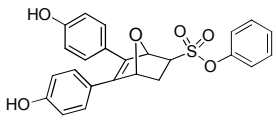	**OBHS**	14.40 ± 1.70	6.93 ± 0.05	2.08	21.53	49.06	2.28

[a]Relative Binding Affinity (RBA) values are determined by competitive flourometric binding assays and are expressed as $IC_{50}^{estradiol} / IC_{50}^{compound} \times 100 \pm$ the range (RBA, estradiol = 100%). [b]K_i values of each conjugate for each receptor were obtained from the RBA values by the formula $K_i = (100/RBA) \times K_d$. The K_d value of estradiol is 3.1 nM for ERα and 3.4 nM for ERβ, respectively. For details, see Experimental Section.

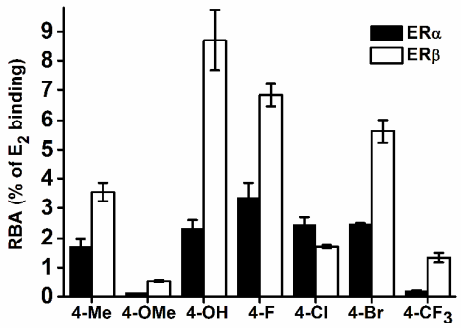

Figure 3. Graphical exhibits RBA values for alternating substituents at 4-position of the phenyl sulfonate moiety.

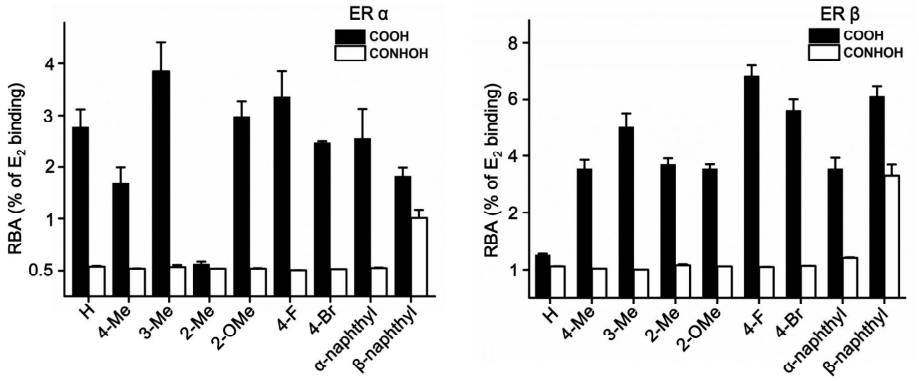

Figure 4. Graphical exhibits RBA values for hydroxamic acid conjugates (**23a-c**, **23f**, **23i-j**, **23m**, **23q-r**) and hydroxamate conjugates (**24a-i**).

Transcription Activation Assays. Various OBHS-HDACi conjugates were tested by an ER-responsive luciferase reporter gene assays for their ability to stimulate the transcriptional activities of ERα and ERβ compared to 17β-estradiol (E_2). Luciferase assays were conducted in HEK 293T cells transfected with a widely used 3 × ERE-luciferase reporter. These results are summarized in Table 4, and dose-response curves for representative samples and reference drug are shown in Figure 5.

Compounds with agonistic activity were usually classified into three groups, normal agonist, partial agonist,[33] or super-agonist,[17] based on their maximum efficacy (Emax) of cell proliferation. The interesting activities are seen in series I. Conjugates possessing a *para*-SAHA group at phenyl sulfonate unit, are potent and highly efficacious ERα and ERβ antagonists; yet, most benzothiophene scaffold-based hybrid HDAC inhibitors (termed SERMostats), developed by Thatcher *et al*, showed little effect on transcriptional activity,[26] and ethynylestradiol-HDACi conjugates (EED-HDACi) developed by Oyelere *et al*, retained the ERα agonist activity of their parent compound EED.[34] Compound **21a** has about a 2-fold improved binding affinity (Table 2, entries 1 vs 3) for ERα, demonstrated about 216-fold higher potency but reduced efficacy as an ERα antagonist (Table 3, entries 1 vs 3), compared to compound **20a**. Compared to OBHS, compound **21a** has higher efficacy as an ERα

antagonist (Table 3, entries 3 vs 33). However, compared to carboxylic acid conjugate **21a** and methyl ester conjugate **20a**, hydroxamic acid analogue **22** had little effect on ERα-mediated transcription. Interestingly, replacing the *para*-SAHA with *meta*-SAHA group gives compounds **20b** and **21b**, which act as partial ERα and ERβ agonists.

Compound **23a**, which bears the SAHA group on the phenol ring, acts as as ERα antagonist. In cases of compound **23a**, however, modifications of the phenyl sulfonate moiety (compounds **23b**-**r**) result in a wide range of activities on ERα or ERβ. Compound **23b**, which has a *para*-methyl on the phenyl sulfonate moiety, acts as an agonist at ERβ and antagonist at ERα. When the methyl group was changed from the *para*- to *meta*-position, compound **23c** showed improved binding affinity for both ERs (Table 2, entry 8), but this had little effect on transcriptional activity. The 2-methyl analogue **23f** displayed increased transcriptional activity on ERα compared to compound **23b**. 4-Methoxyl analogue **23d** showed lower potency as an ERβ agonist, along with weaker binding affinity, compared to the 4-methyl analogue **23b**.

These results demonstrate that very small changes to the phenyl sulfonate moiety can have drastic effects on the potency of these compounds as ERβ agonists. However, the relationship between RBA values and ERβ transcriptional activity is still unclear. For example, 4-hydroxyl derivative **23h** showed about 16-fold improved binding affinity for ERβ, and it stimulated ERβ activity with higher potency compared to **23d**, yet the 3-hydroxyl derivative **23g** showed about 2-fold weaker affinity for ERβ (Table 2, entries 12 vs 13) and was more efficacious than that of estradiol, being about 2-fold more potent as an ERβ superagonist than **23h**.

Introduction of halogens onto the phenyl sulfonate moiety had obvious effects on the transcriptional activity of the ER subtypes. The fluoro analogue **23j** and the chloro analogue **23l** displayed agonist activity at ERα; actually, **23l** profiled as superagonist on ERα, showing efficacy in ERα 1.5 times greater than that of estradiol (Table 3, entry 17), while the bromo analogue **23m** profiled as antagonist on ERα. The trifluoromethyl-substituted compounds **23n**, and **23o** also profiled as ERα antagonist.

Table 3. Effects of OBHS-HDACi Conjugates on the Transcriptional Activities of Estrogen Receptor α and β

		Agonist Mode[a]				Antagonist Mode[b]			
		ERα		ERβ		ERα		ERβ	
entry	cmpd	EC_{50} (μM)	Eff (% E_2)	EC_{50} (μM)	Eff (% E_2)	IC_{50} (μM)	Eff (% E_2)[c]	IC_{50} (μM)	Eff (% E_2)
1	**20a**	-	-35 ± 1	-	4 ± 4	10.8	10 ± 13	0.33	76 ± 18
2	**20b**	0.001	16 ± 5	-	3 ± 4	-	111 ± 13	-	91 ± 17
3	**21a**	-	-10 ± 4	-	-5 ± 1	0.05	25 ± 12	0.16	89 ± 2
4	**21b**	-	51 ± 4	2.1	47 ± 10	-	122 ± 22	-	102 ± 5
5	**22**	-	-15 ± 11	-	3 ± 4	-	104 ± 29	1.14	-27 ± 3
6	**23a**	-	-13 ± 5	0.93	36 ± 10	1.21	36 ± 12	-	97 ± 17
7	**23b**	-	-6 ± 3	0.52	8 ± 3	1.08	36 ± 11	-	111 ± 1
8	**23c**	-	-28 ± 2		-11 ± 17	-	43 ± 1	-	87 ± 15
9	**23d**	-	27 ± 7	-	5 ± 1	115.6	40 ± 27	-	137 ± 20
10	**23e**	1.16	67 ± 3	1.1	100 ± 12	-	87 ± 1	-	100 ± 0
11	**23f**	-	-3 ± 6	0.38	24 ± 3	0.46	43 ± 1	-	117 ± 14
12	**23g**	3.69	77 ± 9	8.1	105 ± 1	-	108 ± 14	-	120 ± 3
13	**23h**	2.42	79 ± 5	13.4	69 ± 28	-	99 ± 12	11.7	23 ± 3
14	**23i**	0.016	84 ± 15	1.8	65 ± 1	-	104 ± 13	0.29	78 ± 7
15	**23j**	18.0	38 ± 6	-	-13 ± 1	-	99 ± 18	0.28	85 ± 5
16	**23k**	-	12 ± 1	-	37 ± 0	0.14	24 ± 4	-	87 ± 5
17	**23l**	0.79	149 ± 22	0.58	44 ± 2	-	93 ± 6	-	188 ± 4
18	**23m**	-	-36 ± 3	-	-3 ± 2	1.7	75 ± 8	0.25	77 ± 15
19	**23n**	-	-51± 7	-	-12 ± 3	0.79	10 ± 3	-	136 ± 7
20	**23o**	-	9 ± 1	-	10 ± 3	0.64	37 ± 15	-	102 ± 5
21	**23p**	0.32	61 ± 23		-8 ± 6		127 ± 42	-	87 ± 12
22	**23q**	-	5 ± 7	-	-13 ± 0.4	0.13	14 ± 9	0.089	15 ± 5
23	**23r**	-	-21 ± 7	0.53	19 ± 1	0.92	45 ± 15	-	94 ± 9
24	**24a**	-	20 ± 5	0.002	38 ± 4	-	77 ± 5	-	92 ± 1
25	**24b**	-	-28 ± 7	0.038	52 ± 10	-	116 ± 3	-	95 ± 2
26	**24c**	-	38 ± 2	0.054	29 ± 6	-	115 ±6	0.613	48 ± 2
27	**24d**	-	-20 ± 5	0.203	27 ± 11	-	126 ± 9	-	94 ± 6
28	**24e**	-	9 ± 2	0.023	53 ± 10	-	164 ± 26	-	74 ± 7
29	**24f**	-	-	0.002	49 ± 1	-	135 ± 1	-	86 ± 4
30	**24g**	1.14	33 ± 9	0.173	21 ± 9	-	101 ± 15	-	91 ± 6
31	**24h**	-	-22 ± 8	-	36 ± 1	-	88 ± 3	-	94 ± 1
32	**24i**	-	13 ± 5	-	-17 ± 7	0.16	-26 ± 5	7.7	19 ± 8
33	**OBHS**	0.095	60 ± 2	-	0 ± 1	0.014	70 ± 12	0.581	-16 ± 2

[a]Luciferase activity was measured in HEK 293T cells transfected with 3 × ERE-driven luciferase reporter and expression vectors encoding ERα or ERβ and treated in triplicate with increasing doses (up to 10^{-5} M) of the compounds. EC_{50} and

standard deviation (mean ± SD), shown as a percentage of 10^{-8} M 17β-estradiol (E_2), were determined. [b]IC_{50} and standard deviation (mean ± SD) were determined in the percentage of 10^{-8} M 17β-estradiol (E_2) on ERα or ERβ. [c]ERs have considerable basal activity in HEK 293T cells; compounds with inverse agonist activity are given negative efficacy values. Omitted EC_{50} or IC_{50} values were too high to be determined accurately.

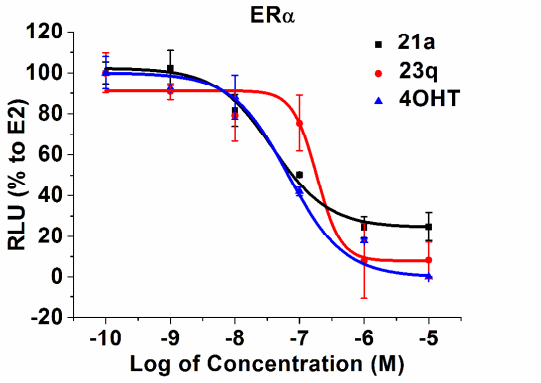

Figure 5. Illustrative dose-response curves for the ERα antagonist effects of 4OHT, and two OBHS-HDACi conjugates **21a** and **23q**. Efficacy values are the mean ± SD from three experiments. For details, see the Experimental Section.

Interestingly, comparisons of the ERα antagonist efficacy of **23a**, **23b**, **23d**, **23h** and **23n** indicate that substituents at the 4-position of the phenyl sulfonate moiety have significant effects. Overall, the electron-withdrawing substituent (CF_3) conveys higher efficacy than the alkyl (methyl) or electron-donating (OMe or OH) groups. Replacing the phenyl with a bulkier group also resulted in marked effects on the transcriptional activity. The 2,6-dimethyl substituent (**23p**) was actually a full agonist of ERα, while those with bulkier substituents, such as, α-naphthyl and β-naphthyl, profiled as ERα antagonists. The α-naphthyl substituent had increased ERα antagonist efficacy with at least 9-fold more potency than **23a** (Table 3, entries 22 vs 6), and the β-naphthyl substituent reduced efficacy, albeit increasing ERα antagonist potency (Table 3, entries 23 vs 6). However, these bulkier substituents displayed lower efficacy than the trifluoromethoxy compound (**23n)**. These results are summarized in Figure 6. The most interesting activities were seen with the hydroxamate conjugates

24a-h. These conjugates had little antagonist potency and efficacy at ERα; however, most of them profiled as partial agonists at ERβ, and showed greater potency than their corresponding carboxylic acid derivatives (Table 3, entries 24-30). Modification of the **23r** by replacing the carboxylic acid group with an hydroxamic acid increased ERα antagonist potency and efficacy (Table 3, **23r** vs **24i**).

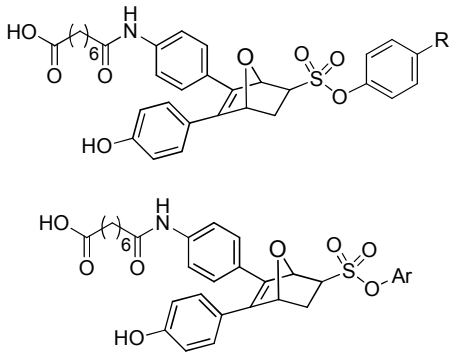

Antagonist Mode

cmpd	R	%Eff. ERα
23a	H	36
23b	Me	36
23d	OMe	40
23h	OH	99
23n	**CF_3**	**10**

	Ar	%Eff. ERα
23p	2,6-diMePh	127
23q	α-naphthyl	14
23r	β-naphthyl	45

Figure 6. Comparisons of ERα antagonistic activities (Eff% of E_2) of series II OBHS-HDACi conjugates. The top tables are for changing substituents of phenyl sulfonate moiety at the 4-position and the bottom tables for replacing the phenyl with a bulkier group.

Structural analysis of the origin of enhanced antagonist character of OBHS-HDACi conjugates. E_2 supports transcriptional activation of ERα and ERβ by stabilizing helix 12 in a position where it forms one side of a hydrophobic groove for binding transcriptional coactivators. The traditional SERMs or full antagonists have typically been developed by adding a bulky side group that directly obstructs the agonist position of helix 12, relocating it out of this position and thereby blocking the recruitment of transcriptional coactivators.[35-37] By contrast, the oxabicyclic core derivatives, such as OBHS, have revealed a novel mechanism of antagonism via small alkyl ester substitutions on the bicyclic core that indirectly modulate the critical switch helix 12, by interactions with helix 11, a process that we have termed "passive antagonism".

Molecular modeling shows that one *para*-hydroxy phenyl group attached to the oxabicyclic core of OBHS (Figure 7A) engages in hydrogen bonding with Glu 353, which mimics the role of A-ring phenol of E_2. The second phenol points in the E_2 11β

direction, but is too short to interact directly with helix 12. The key interaction for antagonism is that of the large, non-poplar phenyl sulfonate group of OBHS, which makes strong steric clashes with helix 11 and indirectly modulates the conformation of the critical helix 12.

Consistent with this model, we find that OBHS-HDACi conjugate **21a** (Figure 7B) can similarly form a hydrogen bond between a phenolic hydroxyl group with Glu 353; moreover, the bulkier sulfonate side chain accentuates this clash with helix 11, thus giving **21a** potent ERα antagonist activity. In contrast, 4-hydroxytamoxifen (Figure 7C) has a bulky side chain that projects between helices 3 and 11, directly displacing helix 12 from its active conformation and destroying the transcriptional coactivator binding site. Compound **23q** (Figure 7D) mimics the binding orientation of 4-hydroxytamoxifen, with the SAHA group not directly interacting with any helix 12 residues, which is consistent with 4-hydroxytamoxifen. Instead, the SAHA side chain of **23q** forms hydrogen bond contacts with helix 3 (Ser 341, Leu 345, and Leu 346) which can induce subtle shifts in helix 3 that destabilize helix 12 and destroy the transcriptional coactivator-binding site, and again thereby reducing the AF2-meditated activity of ERα by an indirect mechanism. Therefore, contact with helix 3 may represent a novel epitope to generate a full ERα antagonist.

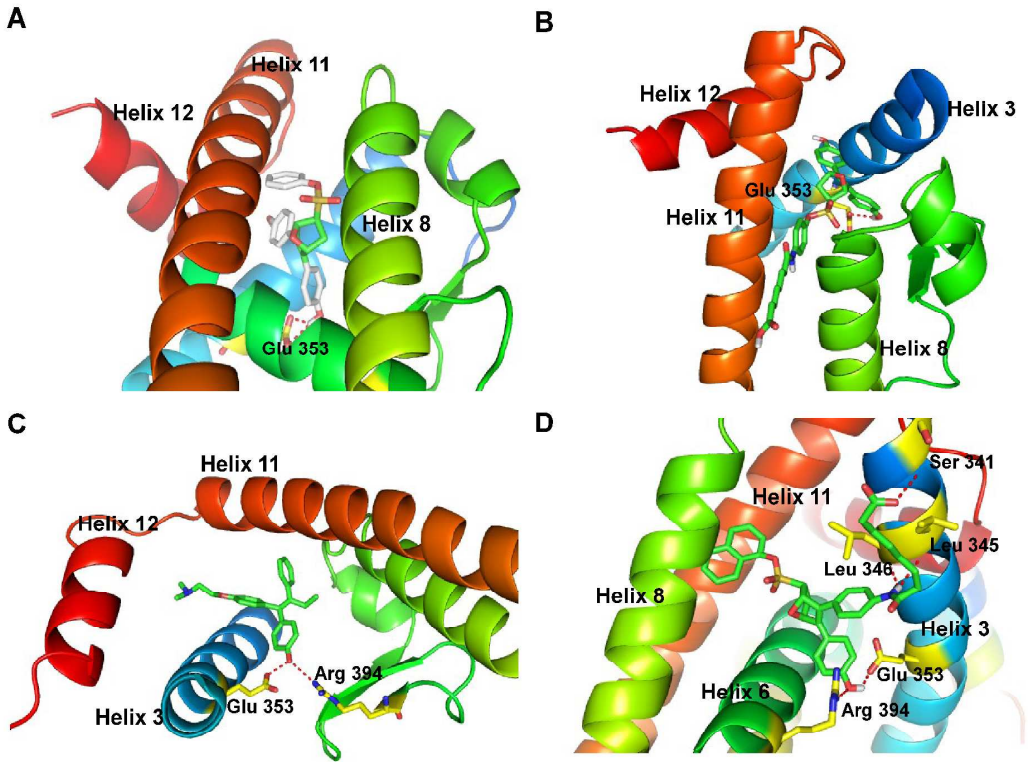

Figure 7. Model of OBHS-HDACi conjugates bound to ERα and comparisons with OBHS and 4-hydroxytamoxifen. (A) Computer-developed model of oxabicyclic heptane sulfonate (OBHS) bound ERα (PDB: 3ERD).[38] OBHS H-bonds to the conserved Glu 353 on helix 3. The phenyl sulfonate binds extends between helices 8 and 11. (B) Computer-developed model of **21a** bound to ERα with the conserved H-bonding to Glu 353, and the sulfonate moiety extending between helices 8 and 11. (C) Crystal structure of the ERα LBD in complex with 4-hydroxytamoxifen (4OHT) (PDB: 3ERT).[39] 4-OHT forms hydrogen bonds with Glu 353 and Arg 394, the side chain displaces helix 12. (D) Computer-developed model of **23q** bound to ERα with the conserved H-bonding to Arg 394, Ser 341, Leu 345, Leu 346 and Glu 353, and the sulfonate moiety extending between helices 8 and 11.

Whole cell antiproliferative activity. To evaluate their anticancer activity, all dual-acting conjugates were screened against MCF-7 (hormone-dependent breast cancer cells), DU-145 (hormone-refractory, metastatic prostate cancer cells), as well as one control cell line, healthy kidney epithelial cells (VERO), and the results are summarized in Table 4. Overall, most OBHS-suberic acid conjugates are much more

potent than lead compound OBHS and corresponding hydroxamic acid conjugates at reducing cancer cell proliferation, despite the fact that OBHS is equipotent to 4OHT against MCF-7 cells. This observation indicates that antiproliferative activity of these OBHS-HDACi conjugates against MCF-7 cells derives mainly from inhibition of ER, and inhibition HDAC can enhance potency against MCF-7 cells. In fact, OBHS does not possess anti-HDAC activity (Table 6, entry 15). Moreover, these carboxylic acid conjugates show enhanced potency against DU-145, unlike the OBHS, which is essentially inactive. This also suggests that the antiproliferative activity against DU-145 of these OBHS-HDACi conjugates comes mainly from HDAC inhibition.

Another interesting aspect of antiproliferative activity is that most conjugates showed significant antiproliferative effects on MCF-7 breast cancer cells, which is greater than those of DU-145 cells. SAHA was also very effective on MCF-7 cells and DU-145 cells. This drug, however, showed low cell-type selectivity, in fact, the majority of HDACi tested clinically exhibit unselective effects on different cell-types, and on-target ineffectiveness.

The compounds **23c**, **23g**, **23l**, and **23q** were equipotent to SAHA but had 5-30-fold greater selectivity than SAHA against MCF-7 cells (Table 4, entries 9 vs 34; 13 vs 34; 18 vs 34; 23 vs 34). The antiproliferative activity of these conjugates on MCF-7 cells was also compared with that of the anti-breast cancer drug 4OHT. The compounds **20b**, **21a**, **23e**, and **23r** were equipotent to 4OHT (Table 4, entries 3 vs 35; 4 vs 35; 11 vs 35; 24 vs 35), while these four compounds showed about 2-3 fold greater selectivity than 4OHT in favor of MCF-7 cells.

Most encouragingly, seven compounds, **20a**, **23c-d**, **23f-g**, **23l**, **23q**, exhibited more potent antiproliferative activity than 4OHT. Specifically, compound **23l** shows about 5-fold greater potency than 4OHT (IC_{50} = 3.3 μM, against MCF-7 cells) and over 30-fold greater selectivity for MCF-7 cells over DU-145 cells (Table 4, entries 18 vs 35), although it showed low binding affinity to both ERs. This suggests that binding affinity and antiproliferative potency are independent. This conclusion was also confirmed by compound **23h**, which possessed high binding affinity with, however, no inhibition of either MCF-7 or DU-145 cells.

Table 4. Whole cell antiproliferative activity (IC_{50}, μM)[a]

Entry	Compound	MCF-7	DU-145	VERO
1	**OBHS**	20.9 ± 1.00	>100 [b]	>100
2	**20a**	8.1 ± 0.77	20.4 ± 1.92	>100
3	**20b**	19.1 ± 1.09	19.3 ± 5.82	>100
4	**21a**	19.1 ± 4.06	34.8 ± 2.91	>100
5	**21b**	>100	> 100	>100
6	**22**	55.2 ± 0.86	42.3 ± 1.54	>100
7	**23a**	66.4 ± 2.09	> 100	>100
8	**23b**	60.5 ± 2.09	80.8 ± 6.02	>100
9	**23c**	3.8 ± 0.69	52.4 ± 1.35	>100
10	**23d**	15.3 ± 0.10	38.6 ± 8.32	>100
11	**23e**	17.9 ± 1.94	53.8 ± 3.88	>100
12	**23f**	7.9 ± 1.36	> 100	>100
13	**23g**	3.6 ± 0.29	23.8 ± 7.29	>100
14	**23h**	> 100	> 100	>100
15	**23i**	> 100	> 100	>100
16	**23j**	24.8 ± 1.23	> 100	>100
17	**23k**	27.9 ± 2.46	27.7 ± 3.70	>100
18	**23l**	3.3 ± 0.83	> 100	>100
19	**23m**	>100	> 100	>100
20	**23n**	24.0 ± 2.11	77.0 ± 9.29	>100
21	**23o**	26.1 ± 6.05	> 100	>100
22	**23p**	> 100	> 100	>100
23	**23q**	4.7 ± 1.68	48.6 ± 2.46	>100
24	**23r**	18.9 ± 1.73	58.3 ± 13.7	>100
25	**24a**	30.1 ± 3.59	37.7 ± 7.55	>100
26	**24b**	40.4 ± 1.41	42.9 ± 2.40	>100
27	**24c**	22.9 ± 2.23	32.2 ± 1.08	>100
28	**24d**	24.1 ± 2.63	30.7 ± 6.56	>100
29	**24e**	25.8 ± 2.76	44.7 ± 2.34	>100
30	**24f**	23.4 ± 2.64	47.3 ± 0.79	>100
31	**24g**	17.13 ± 1.79	11.3 ± 3.18	>100
32	**24h**	13.4 ± 0.94	8.57 ± 0.57	>100
33	**24i**	32.2 ± 1.32	12.4 ± 1.66	>100
34	**SAHA**	2.50 ± 0.33	1.2 ± 0.07	4.1 ± 0.19
35	**4OHT**	15.6 ± 1.77	15.3 ± 4.42	15.1 ± 5.21

[a] IC_{50} values are an average of at least three independent experiments ± standard deviation (mean ± SD). [b] IC_{50} not determinable up to highest concentrations tested.

A closer analysis of the cell growth inhibition data in Table 4 revealed that the hydroxamate compounds (**24a-i**) also showed significant antiproliferative effects on MCF-7 breast cancer cells. The conjugates **24a-b**, **23i**, and **24d** show enhanced

potency against MCF-7 cells, compared to **23a-b**, **23i**, **23m**. Interestingly, the general trend of conjugates against MCF-7 cells still is that carboxylic acid conjugates are more potent than hydroxamate compounds. For example, compound **24h** stands out among these hydroxamate compounds, while **24h** is about 4-fold less potent than **23l**. Another interesting aspect of the antiproliferative activity is that these hydroxamate conjugates (**24a-i**) were more potent than their corresponding carboxylic acid conjugates, against DU-145. Compound **24h** shows the greatest potency against DU-145 cells because it shows a good HDAC6 inhibition profile (Table 6, entry 12).

Additionally, all conjugates are nontoxic to healthy VERO cells, while SAHA and 4OHT showed considerable toxicity. In fact, some Tam-HDACi conjugates are still toxic to the healthy VERO cells.[34] Comparing the activity of conjugates (**20a-b**, **21a**, **23c-g**, **23l**, **23n**, **23q-r**) with control drugs SAHA and tamoxifen on VERO, 4OHT had the smallest *in vitro* therapeutic index (IVTI), while our conjugates show greater IVTIs (Table 5).

Table 5. *In vitro* therapeutic index (IVTI) of OBHS-HDACi conjugates 20a-b, 21a, 23c-g, 23l, 23n, and 23q-r.

Compound	*IVTI*[a]	Compound	*IVTI*
20a	> 12.34	**23f**	> 12.66
20b	> 5.24	**23g**	> 27.78
21a	> 5.24	**23l**	> 30.3
23c	> 26.2	**23n**	> 4.17
23d	> 6.54	**23q**	> 21.28
23e	> 5.59	**23r**	> 5.29
SAHA	1.64	**4OHT**	0.97

[a] IVTI = IC_{50}(VERO) / IC_{50}(MCF-7).

Conjugates Exhibit Potent HDAC Inhibition Activity. As a final test, an array of representative OBHS-HDACi conjugates with significant antiproliferative effects on both MCF-7 and DU-145 cell lines were assayed for HDAC inhibition activity against HDAC1, and HDAC6 (Table 6). Although these three isoforms, HDAC1, HDAC6,

and HDAC8, have been implicated in breast tumor,[40] recently, HDAC1 and HDAC6 have been found to be more critical in breast cancer cells.[26, 34] Conjugates **20a** and **21a** of series I strongly inhibit HDAC1 and HDAC6, and demonstrate high selectivity for HDAC1 (with nanomolar range of IC_{50}) over HDAC6. Interestingly, replacing carboxylic acid of **21a** with hydroxamic acid led to dual-preference for each HDAC isoform. Actually, hydroxamic acid compounds SAHA and **24i** also exhibit roughly equal inhibition against HDAC1 and HDAC6.

When a suberic acid or SAHA group is appended onto one of phenol ring, in general, conjugates are more selective for HDAC6, having modest or no activity against HDAC1 (Table 6, entries 5, 7, 9-10, 12-13). The effect of modification of the phenyl sulfonate moiety is also dramatic: e.g., introduction of a 4-methoxyl substituent on the phenyl ring, compound **23d**, produces a weaker inhibitor for HDAC1, too weak, in fact, to make an accurate measurement of the IC_{50} value. However, a change from the 3-methyl (**23c**) to the 2-methyl (**23f**) results in at least 130-fold increase in potency for HDAC1 (entry 6). It is noteworthy that among all conjugates, the **23f** shows the most potent anti-HDAC1 (IC_{50} = 22 nM) activity. It is 2-fold more potent than the SAHA in HDAC1 inhibition (entry 16), which is equipotent to EED-HDACi conjugates, and more potent than SERMostats and Tam-HDAC conjugates.[26, 34] When 3-methyl (**23c**) is changed to the hydroxyl group (**23g**) it results in at least 140-fold increase in potency for HDAC6, giving it half of inhibitory activity of that of SAHA (entry 7). In contrast, the 4-methoxyl, the 4-chloro and 4-triflouromethyl analogues **23d**, **23l** and **23n** also display good inhibition preference for HDAC6. Interestingly, although **23l** is an ER agonist, which has even more promising antiproliferative activity against MCF-7 (Table 4, entry 18), and also shows strong inhibition activity against HDAC1 (IC_{50} = 241 nM, entry 8). This observation suggests that the enhancement of antiproliferative activity of **23l** against MCF-7 derives mainly from HDAC inhibition. However, replacement of the phenyl group of sulfonate moiety with the bulkier α-naphthyl group (**23q**) results in no detectable inhibitory activity for HDAC1 and HDAC6. Interestingly, when the α-naphthyl group is replaced by a β-naphthyl group, compound **23r** is surprising by

showing IC_{50} values of 0.282 μM and 8.11 μM for HDAC1 and HDAC6, respectively (entry 11). When the carboxylic acid group of **21a**, **23q-r** is converted to corresponding hydroxamate (**22**, **24h-i**), the potency for HDAC1 usually decreased, but there is at least 25-fold increase in inhibition for HDAC6 (Table 6, entries 2 vs 3; 10 vs 13; 11 vs 14). Compound **24g** also shows no inhibition for HDAC1, but displays modest potency for HDAC6 (entry 12). The parent compound OBHS, which is essentially inactive for either of HDACs (entry 15).

Table 6. IC_{50} values of representative conjugates for inhibition of HDAC1 and HDAC6.

Entry	Compd		HDAC1 [μM]	HDAC6 [μM]
1	**20a**	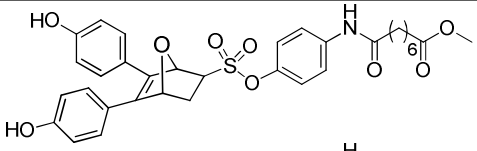	0.534	1.58
2	**21a**	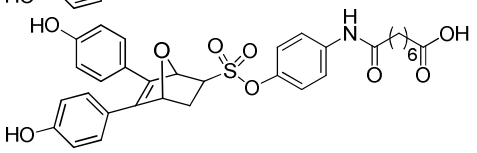	0.107	8.34
3	**22**	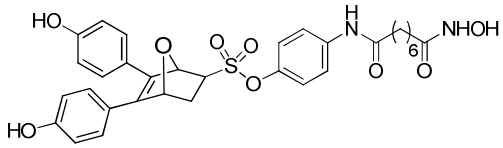	0.583	0.189
4	**23c**	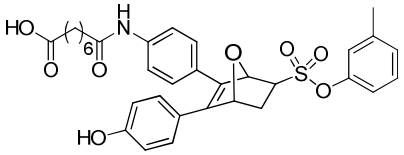	2.98	ND
5	**23d**	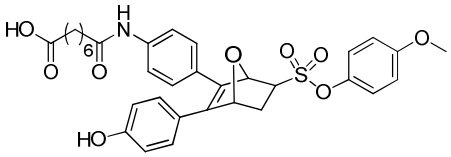	ND	4.17
6	**23f**	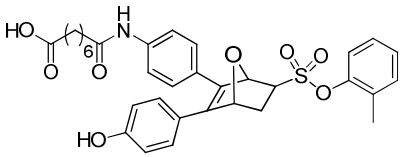	0.022	5.01
7	**23g**	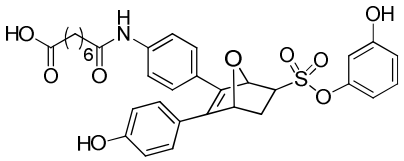	ND	0.071
8	**23l**	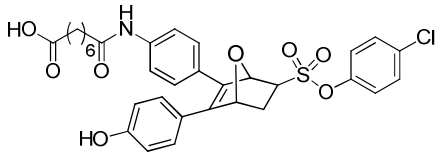	0.241	1.46
9	**23n**	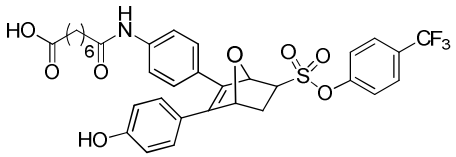	ND	0.648

Table 6. Continued

Entry	Compd		HDAC1 [μM]	HDAC6 [μM]
10	**23q**	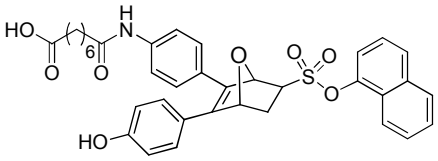	ND	ND
11	**23r**	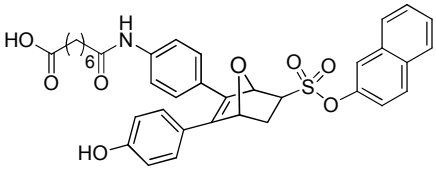	0.282	8.11
12	**24g**	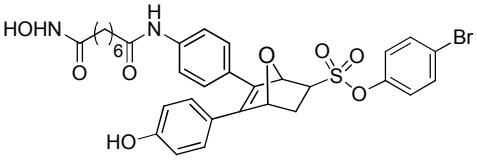	ND	0.23
13	**24h**	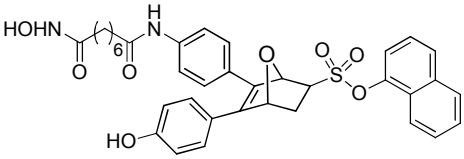	ND	0.03
14	**24i**	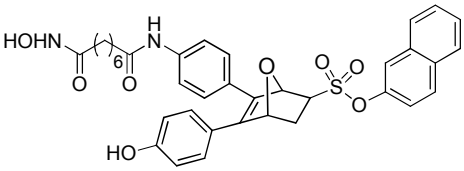	0.349	0.322
15	**OBHS**	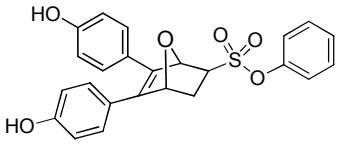	ND	ND
16	**Vorinostat (SAHA)**	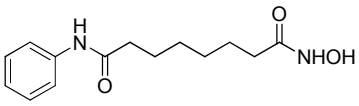	0.0474	0.0297

[a]ND = inhibition not detectable.

CONCLUSIONS

Cancer is a highly complex multigenetic and multifactorial disease. Combination therapy that combines multiple drugs working through different mechanisms is a proven therapeutic strategy for disease management, including breast cancer, and in particular a synergistic effect of combined tamoxifen and HDACi on ERα-positive breast cancer cells has been seen.[41, 42] Although drug cocktails exhibit various advantages, such as avoidance of drug resistance, the outcome from traditional

combination therapy involving estrogen modulators and HDAC inhibitors remains complicated by the inherently different pharmacokinetic profile of the two separate drugs. The recent clinical trials also indicate that combination therapy of some anticancer drugs has been suspended due to the high toxicity.[43] In contrast, the hybrid chemotherapeutic agents, which combine two complementary bioactive units within a single molecule, might have more beneficial effects and fewer side effects than single-target agents via simultaneously modulating multiple targets and circumventing differences in pharmacokinetic profiles.

In order to further explore anti-breast cancer drugs that might have superior efficacy and fewer side effects than tamoxifen or other therapeutic agents, it was of interest to develop agents that possess ERα antagonist and HDAC inhibitory activities in a single molecule. To this end, we have successfully synthesized two novel Series of dual-action conjugates targeting ER and HDAC simultaneously. These conjugates exhibited very good ER binding affinity, and excellent antagonist activity on ERα. Careful analysis of their ER binding affinity output showed that the series I conjugates are largely ERα-selective, collectively, and the series II conjugates are largely ERβ-selective.

While conversion of the carboxylic acid to an hydroxamic acid resulted in a sharp decrease in ER binding affinity and ERα antagonist potency, compared with the approved anti-breast cancer drug tamoxifen, most of conjugates exhibited superior antitumor potency and cell-type selectivity in breast cancer MCF-7 cell lines. Moreover, all conjugates are nontoxic to health VERO cells, while SAHA and tamoxifen each alone showed, at least to some extent, inherent toxicity. The most promising compound of this study, **21a**, has the highest binding affinity for ERα and also exhibits partial ERα antagonist activity in transcription assays; its antitumor potency in breast cancer MCF-7 cells is equipotent to that of 4OHT, and it strongly inhibits HDAC1 and HDAC6, with some selectivity for the former enzyme. These results were also supported by a model of the **21a** bound to ERα, in which the carboxylic acid side chain on the phenyl sulfonate group of OBHS accentuates the clash of this portion of the molecule with helix 11, an interaction that might be

responsible for its increased antagonistic efficacy for ERα and its potent antitumor potency in breast cancer MCF-7 cell. Therefore, in terms of the mechanism of action of these conjugates, we suspect that these dual-targeting compounds maybe functioning in a "serial fashion", first binding to the ER target, which localizes them in ER(+) tissues and then subsequently inhibiting HDACs after dissociation from ER.

Lastly, compound **23f** shows the most potent anti-HDAC1 (IC_{50} = 22 nM) activity, which is 2-fold more potent than that of the clinical agent SAHA inhibition of HDAC1, and it is equipotent to EED-HDACi conjugates, while being more potent than SERMostats and Tam-HDAC conjugates.

Thus, the OBHS-HDACi conjugates represent a novel approach to the development of efficient estrogen receptor antagonists via the concept of unique SERM and HDAC inhibitor hybrids for breast cancer therapy. An in-depth mechanistic study of these compounds with ER is still ongoing in our laboratory and will be reported in a due course.

EXPERIMENTAL SECTION

Materials and Methods. Unless otherwise noted, starting materials were purchased from commercial suppliers and were used without further purification. Tetrahydrofuran (THF) was dried over Na and distilled prior to use. Dichloromethane and triethylamine were dried over CaH_2 and distilled prior to use. Glassware was oven-dried, assembled while hot, and cooled under an inert atmosphere. All reactions were performed under an argon atmosphere unless otherwise specified. Reaction progress was monitored using analytical thin-layer chromatography (TLC). Visualization was achieved by UV light (254 nm). ^{1}H NMR and ^{13}C NMR spectra were measured on a Bruker Biospin AV400 (400 MHz) instrument. Chemical shifts are reported in ppm (parts per million) and are referenced to either tetramethylsilane or the solvent. The purity of all compounds for biological testing was determined by HPLC method (see Supporting Information), confirming > 95% purity.

General Procedure for Diels-Alder Reaction (20a-b, 21a-b, 23a-r).

Furan **4** or **12** (0.7 mmol) and dienophile(**16a-b**, **19a-r**, 0.84 mmol) were in a round flask, and the reaction mixture was stirred at 90 °C for 12h. The crude product was

purified by silica gel column chromatography (Dichlormethane-MeOH, 60 : 1~30 : 1).

General Procedure for hydroxamic acid derivatives (22, 24a-i).

To a 0 °C cooled solution of carboxylic acid derivative (**21a, 23a-c, 23f, 23i-j, 23m, 23q-r,** 0.16 mmol) in dry THF (25 mL), ethyl chloroformate (29.4 mg, 0.24 mmol) and triethylamine (27.3 mg, 0.27 mmol) were added and the mixture was stirred for 15 min. The precipitate was filtered off and the filtrate was added to frshly prepared soluton of hydoxylamine in methanol. To prepare the hydroxylamine, a solution of hydroxylamine hydrochloride (333.6 mg, 4.8 mmol) in in methanol (15 mL), potasium hydroxide (268.8 mg, 4.8 mmol) was added at 40 °C for 15 min. The reaction mixture was cooled to 0 °C, the precipitate was filtered off, and the filtrate was used as such. The resulting mixture was was stirred for 1h and then was evaporated, and the residue was purified by silica gel column chromatography (Dichlormethane-MeOH, 30 : 1) to give corresponding hydroxamic acid (**22, 24a-i**).

Methyl 8-(4-(5,6-bis(4-Hydroxyphenyl)-7-oxabicyclo[2.2.1]hept-5-en-2-yl sulfonyloxy)phenyl amino)-8-oxooctanoate (20a). White solid, 91% yield, m.p. 99-101 °C; ^{1}H NMR (400 MHz, Acetone-d_6) δ 7.53 (d, J = 9.2 Hz, 2H), 7.12 (m, 6H), 6.74 (d, J = 8.4 Hz, 2H), 6.66 (d, J = 8.8 Hz, 2H), 5.57 (s, 1H), 5.34 (d, J = 4.0 Hz, 1H), 4.09 (m, 2H) , 3.66 (m, 1H), 3.60 (m, 3H), 2.31 (m, 4H), 1.65 (m, 2H), 1.58 (m, 2H), 1.34 (m, 4H). ^{13}C NMR (100 MHz, Acetone-d_6) δ 175.98, 174.63, 158.91, 158.77, 146.51, 142.52, 139.02, 138.02, 130.33, 129.73, 125.13, 124.40, 123.69, 122.25, 116.81, 116.56, 85.82, 84.18, 61.58, 52.03, 37.86, 34.73, 31.63, 29.95, 29.89, 25.87, 20.93; HRMS (ESI) calcd for $C_{33}H_{36}NO_9S$ $[M + H]^+$, 622.2107; found 622.2105.

Methyl8-(3-(5,6-bis(4-Hydroxyphenyl)-7-oxabicyclo[2.2.1]hept-5-en-2-yl sulfonyloxy)phenyl amino)-8-oxooctanoate (20b). White solid, 89% yield, m.p. 133-135 °C; ^{1}H NMR (400 MHz, Acetone-d_6) δ 9.30 (s, 1H, -CONH-), 8.63 (s, 2H, -OH), 7.79 (s, 1H), 7.60 (d, J = 8.0 Hz, 1H), 7.30 (d, J = 8.4 Hz, 1H), 7.22 (m, 4H), 6.95 (d, J = 8.4 Hz, 1H), 6.83 (m, 4H), 5.64 (s, 1H), 5.45 (d, J = 4.0 Hz, 1H), 3.83 (m, 1H) , 3.60 (s, -OMe), 2.45 (m, 1H), 2.40 (t, J = 7.6 Hz, 2H), 2.30 (m, 3H),1.65 (m,

2H), 1.55 (m, 2H), 1.35 (m, 4H). ^{13}C NMR (100 MHz, Acetone-d_6) δ 174.18, 172.38, 158.36, 158.32, 150.65, 142.32, 141.86, 137.98, 130.71, 129.96, 129.62, 125.03, 124.30, 118.33, 117.35, 116.57, 116.42, 113.89, 85.20, 83.71, 61.79, 51.53, 37.62, 34.27, 31.54, 29.57, 29.32, 25.92, 25.51; HRMS (ESI) calcd for $C_{33}H_{36}NO_9S$ [M + H]$^+$, 622.2107 ; found 622.2105.

8-(4-(5,6-Bis(4-hydroxyphenyl)-7-oxabicyclo[2.2.1]hept-5-en-2-ylsulfonyloxy)phenylamino)-8-oxooctanoic Acid (21a). To a solution of **20a** (150.6 mg, 0.24 mmol) in MeOH (2 mL), a solution of potassium hydroxide (10 mL, 2 mol/L) was added and stirred at room temperature for 3h. After that, acidified by 3% HCl to pH 5, and extracted with ethyl acetate (3 × 25 mL). The extracts were dried (Na_2SO_4) and evaporated. The crude product was purified by silica gel column chromatography (Dichlormethane-MeOH, 30 : 1). White solid, 86% yield, m.p. 87-89 °C; ^{1}H NMR (400 MHz, Acetone-d_6) δ 7.55 (d, J = 8.8 Hz, 2H), 7.17 (m, 6H), 6.77 (d, J = 8.0 Hz, 2H), 6.72 (d, J = 8.4 Hz, 2H), 5.59 (s, 1H), 5.38 (d, J = 4.4 Hz, 1H), 3.67 (m, 1H) , 2.41 (m, 3H), 2.26 (m, 2H), 2.16 (m, 1H), 1.69 (m, 2H), 1.61 (m, 2H), 1.40 (m, 4H). ^{13}C NMR (100 MHz, Acetone-d_6) δ 176.28, 173.23, 157.47, 157.32, 145.09, 141.11, 137.57, 136.59, 128.85, 128.24, 123,68, 122.95, 122.18, 120.84, 115.35, 115.09, 84.39, 82.73, 60.15, 36.4, 33.47, 30.17, 28.54, 28.48, 25.22, 24.50; HRMS (ESI) calcd for $C_{32}H_{34}NO_9S$ [M + H]$^+$, 608.1953; found 608.1949.

8-(3-(5,6-Bis(4-hydroxyphenyl)-7-oxabicyclo[2.2.1]hept-5-en-2-ylsulfonyloxy)phenylamino)-8-oxooctanoic Acid (21b). The process was performed as done in the preparation of **21a** using **20b** instead of **20a** to afford acid **21b**. White solid, 86% yield, m.p. 118-120 °C; ^{1}H NMR (400 MHz, Acetone-d_6) δ 9.30 (s, 1H, -CONH-), 7.79 (s, 1H), 7.57 (d, J = 8.0 Hz, 1H), 7.30 (d, J = 8.4 Hz, 1H), 7.25 (m, 4H), 6.97 (d, J = 8.0 Hz, 1H), 6.81 (m, 4H), 5.64 (s, 1H), 5.44 (d, J = 4.0 Hz, 1H), 3.85 (m, 1H), 2.44 (m, 1H), 2.42 (t, J = 7.6 Hz, 2H), 2.28 (m, 3H), 1.71 (m, 2H), 1.61 (m, 2H), 1.39 (m, 4H). ^{13}C NMR (100 MHz, Acetone-d_6) δ 174.72, 172.32, 158.36, 158.32, 150.66, 142.35, 141.90, 137.99, 130.69, 129.95, 129.61, 125.04, 124.30, 118.28, 117.30, 116.56, 116.40, 113.85, 85.19, 83.70, 61.77, 37.62, 34.12, 31.54, 29.63, 29.57, 25.94, 25.50; HRMS (ESI) calcd for $C_{32}H_{34}NO_9S$ [M + H]$^+$, 608.1953; found 608.1949.

4-(8-(Hydroxyamino)-8-oxooctanamido)phenyl5,6-bis(4-hydroxyphenyl)-7-oxabicyclo[2.2.1]hept-5-ene-2-sulfonate (22). White solid, 56% yield, m.p. 81-83 °C; ^{1}H NMR (400 MHz, CD_3OD) δ 7.54 (d, J = 8.8 Hz, 2H), 7.16 (m, 6H), 6.75 (d, J = 8.4 Hz, 2H), 6.70 (d, J = 8.4 Hz, 2H), 5.58 (s, 1H), 5.38 (d, J = 3.6 Hz, 1H), 3.64 (m, 1H) , 2.37 (m, 3H), 2.18 (m, 1H), 2.08 (t, J = 7.6 Hz, 2H), 1.66 (m, 2H), 1.62 (m, 2H), 1.37 (m, 4H). ^{13}C NMR (100 MHz, CD_3OD) δ 173.21, 171.91, 158.12, 157.51, 145.09, 141.02, 137.57, 136.36, 130.70, 128.85, 128.19, 123.43, 122.19, 120.81, 115.59, 115.56, 115.26, 115.23, 84.40, 82.72, 60.09, 36.36, 32.24, 30.18, 28.45, 28.37, 25.19, 25.16; HRMS (ESI) calcd for $C_{32}H_{34}NNaO_9S$ $[M + Na]^+$, 645.1897; found 645.1893.

8-(4-(3-(4-Hydroxyphenyl)-6-(phenoxysulfonyl)-7-oxabicyclo[2.2.1]hept-2-en-2-yl) phenylamino)-8-oxooctanoic Acid (23a). Pale yellow solid, 95% yield, m.p. 91-93 °C; ^{1}H NMR (400 MHz, Acetone-d_6) δ 9.42 (s, 1H), 7.68 (t, J = 8.8 Hz, 2H), 7.41 (m, 1H), 6.86 (d, J = 8.4 Hz, 7H), 6.83 (d, J = 8.4Hz, 1H), 5.69 (s, 1H), 5.46 (t, J = 3.2 Hz, 1H), 3.60 (s, 1H), 3.34 (s, 1H), 2.42 (m, 2H), 2.27 (m, 2H), 1.69 (m, 2H), 1.59 (m, 2H), 1.37 (m, 4H). ^{13}C NMR (100 MHz, Acetone-d_6) δ 174.40, 172.65, 158.84 158.60, 150.53, 141.85, 139.25, 137.47, 130.87, 130.27, 129.66, 129.03, 128.41, 128.13, 124.52, 123.74, 123.17, 123.15, 120.34, 120.13, 116.83, 116.47, 85.28, 83.70, 61.63, 51.66, 37.69, 34.33, 31.43, 31.33, 26.17, 25.53; HRMS (ESI) calcd for $C_{32}H_{32}NO_8S$ $[M - H]^-$, 590.1862; found 590.1859.

8-(4-(3-(4-Hydroxyphenyl)-6-(p-tolyloxysulfonyl)-7-oxabicyclo[2.2.1]hept-2-en-2-yl)phenylamino)-8-oxooctanoic Acid (23b). Pale yellow solid, 94% yield, m.p. 106-107 °C; ^{1}H NMR (400 MHz, Acetone-d_6) δ 9.33 (s, 1H), 7.67 (t, J = 8.8 Hz, 2H), 7.31 (d, J = 8.4 Hz, 2H), 7.26 (t, J = 8.0 Hz, 2H), 7.16 (m, 4H), 5.67 (s, 1H), 5.46 (t, J = 3.2 Hz, 1H), 3.80 (m, 1H), 2.39 (m, 3H), 2.30 (s, 3H), 2.28 (m, 2H), 1.69 (m, 2H), 1.60 (t, J = 6.4 Hz, 2H), 1.37 (m, 4H). ^{13}C NMR (100 MHz, Acetone-d_6) δ 175.04, 172.49, 158.60, 158.41, 148.45, 143.48, 141.82, 139.34, 137.83, 131.21, 130.20, 129.61, 129.07, 128.43, 124.68, 123.88, 122.58, 120.40, 116.64, 116.45, 85.29, 83.63, 61.21, 37.79, 34.34, 31.53, 31.34, 29.65, 26.27, 25.62, 20.69; HRMS (ESI) calcd for $C_{33}H_{34}NO_8S$ $[M - H]^-$, 604.2015 ; found 604.2011.

8-(4-(3-(4-Hydroxyphenyl)-6-(m-tolyloxysulfonyl)-7-oxabicyclo[2.2.1]hept-2-en-2

-yl)phenyl amino)-8-oxooctanoic Acid (23c). Pale yellow solid, 92% yield, m.p. 94-96 °C; ^{1}H NMR (400 MHz, CD_3OD) δ 7.52 (d, J = 8.4 Hz, 2H), 7.27 (m, 4H), 7.18 (d, J = 8.4 Hz, 2H), 7.06 (t, J = 8.4 Hz, 1H), 6.93 (m, 1H), 6.76 (t, J = 8.4 Hz, 2H), 5.65 (s, 1H), 5.38 (t, J = 4.4 Hz, 1H), 3.85 (m, 1H), 3.62 (d, J = 11.2 Hz, 3H), 2.48 (m, 1H), 2.36 (t, J = 7.2 Hz, 2H), 2.25 (m, 3H), 1.71 (t, J = 6.8 Hz, 2H), 1.61 (t, J = 6.8 Hz, 2H), 1.39 (m, 4H). ^{13}C NMR (100 MHz, CD_3OD) δ 173.28, 173.13, 157.71, 151.60, 143.02, 140.90, 138.38, 138.19, 136.23, 128.89, 128.56, 127.88, 127.65, 127.34, 123.46, 120.44, 119.99, 119.75, 115.41, 115.24, 112.91, 112.88, 84.31, 82.72, 61.37, 54.90, 36.51, 34.89, 30.09, 28.65, 28.59, 25.32, 25.06; HRMS (ESI) calcd for $C_{33}H_{34}NO_8S$ $[M - H]^-$, 604.2012; found 606.2011.

8-(4-(3-(4-Hydroxyphenyl)-6-(4-methoxyphenoxysulfonyl)-7-oxabicyclo[2.2.1]he pt-2-en-2-yl)phenylamino)-8-oxooctanoic acid (23d). White solid, 92% yield, m.p. 108-110 °C; ^{1}H NMR (400 MHz, CD_3OD) δ 7.54 (t, J = 8.4 Hz, 2H), 7.24 (d, J = 8.4 Hz, 2H), 7.16 (d, J = 8.8 Hz, 2H), 7.10 (d, J = 8.8 Hz, 1H), 7.07 (d, J = 9.6 Hz, 1H), 6.80 (m, 4H), 5.61 (s, 1H), 5.38 (t, J = 4.8 Hz, 1H), 3.73 (s, 3H, -OMe), 3.67 (m, 1H), 2.38 (m, 3H), 2.27 (t, J = 7.2 Hz, 2H), 2.20 (m, 1H), 1.69 (m, 2H), 1.61 (m, 2H), 1.38 (m, 4H). ^{13}C NMR (100 MHz, CD_3OD) δ 174.75, 174.72, 159.84, 159.21, 159.05, 144.03, 142.00, 139.78, 137.48, 130.65, 129.93, 129.39, 128.68, 124.28, 123.96, 121.45, 121.17, 116.96, 116.71, 115.85, 115.82, 85.85, 84.06, 61.28, 56.20, 38.22, 35.88, 31.65, 30.08, 27.15, 26.80; HRMS (ESI) calcd for $C_{33}H_{36}NO_9S$ $[M + H]^+$, 622.2101; found 622.2105.

8-(4-(3-(4-Hydroxyphenyl)-6-(3-methoxyphenoxysulfonyl)-7-oxabicyclo[2.2.1]he pt-2-en-2-yl)phenylamino)-8-oxooctanoic Acid (23e). Pale yellow solid, 89% yield, m.p. 97-99 °C; ^{1}H NMR (400 MHz, Acetone-d_6) δ 9.36 (s, 1H), 7.69 (t, J = 8.0 Hz, 2H), 7.32 (t, J = 8.0 Hz, 2H), 7.28 (m, 3H), 6.88 (m, 5H), 5.73 (s, 1H), 5.47 (t, J = 3.6 Hz, 1H), 3.89 (m, 1H), 3.75 (s, 3H, -OMe), 2.49 (m, 1H), 2.42 (t, J = 7.2 Hz, 2H), 2.33 (t, J = 7.6 Hz, 2H), 2.07 (m, 1H), 1.71 (m, 2H), 1.62 (m, 2H), 1.37 (m, 4H). ^{13}C NMR (100 MHz, Acetone-d_6) δ 175.65, 172.99, 161.72, 158.63, 151.32, 143.67, 141.95, 139.31, 137.51, 131.25, 130.27, 129.74, 129.04, 128.46, 124.68, 123.85, 120.47, 116.73, 116.56, 114.98, 113.70, 109.09, 85.19, 83.69, 61.55, 56.06, 37.81,

34.33, 30.85, 29.68, 26.24, 25.55, 20.68; HRMS (ESI) calcd for $C_{33}H_{34}NO_9S$ $[M - H]^-$, 620.1970; found 620.1967.

8-(4-(3-(4-Hydroxyphenyl)-6-(o-tolyloxysulfonyl)-7-oxabicyclo[2.2.1]hept-2-en-2-yl)phenylamino)-8-oxooctanoic Acid (23f). Pale yellow solid, 91% yield, m.p. 94-96 °C; ^{1}H NMR (400 MHz, Acetone-d_6) δ 9.32 (s, 1H), 7.68 (t, J = 8.0 Hz, 2H), 7.35 (m, 6H), 7.26 (m, 2H), 6.82 (t, J = 8.4 Hz, 2H), 5.72 (s, 1H), 5.50 (t, J = 3.6 Hz, 1H), 3.91 (m, 1H), 2.56 (m, 1H), 2.41 (t, J = 7.2 Hz, 2H), 2.32 (d, J = 2.8 Hz, 3H), 2.29 (t, J = 7.2 Hz, 2H), 2.06 (m, 1H), 1.71 (t, J = 6.8 Hz, 2H), 1.58 (t, J = 6.8 Hz, 2H), 1.38 (m, 4H). ^{13}C NMR (100 MHz, Acetone-d_6) δ 175.58, 172.51, 158.66, 148.88, 143.62, 141.99, 140.23, 139.32, 137.63, 132.64, 130.17, 129.79, 128.93, 128.56, 128.09, 127.88, 124.68, 123.94, 123.08, 120.35, 116.69, 116.53, 85.31, 83.26, 62.43, 37.74, 34.26, 31.62, 30.71, 29.66, 26.16, 25.55, 16.92; HRMS (ESI) calcd for $C_{33}H_{35}NO_8S$ $[M + H]^+$, 606.2154; found 606.2156.

8-(4-(6-(3-Hydroxyphenoxysulfonyl)-3-(4-hydroxyphenyl)-7-oxabicyclo[2.2.1]hept-2-en-2-yl)phenylamino)-8-oxooctanoic Acid (23g). Pale yellow solid, 76% yield, m.p. 114-117 °C; ^{1}H NMR (400 MHz, Acetone-d_6) δ 9.38 (s, 1H), 7.67 (t, J = 8.4 Hz, 2H), 7.33 (d, J = 8.8 Hz, 2H), 7.24 (d, J = 8.4 Hz, 2H), 7.19 (m, 1H), 6.87 (t, J = 8.0 Hz, 4H), 6.75 (t, J = 8.4 Hz, 1H), 5.71 (s, 1H), 5.46 (t, J = 3.6 Hz, 1H), 3.88 (m, 1H), 2.49 (m, 1H), 2.46 (t, J = 7.2 Hz, 2H), 2.29 (t, J = 7.2 Hz, 2H), 2.08 (m, 1H), 1.72 (t, J = 6.8 Hz, 2H), 1.61 (t, J = 6.8 Hz, 2H), 1.37 (m, 4H). ^{13}C NMR (100 MHz, Acetone-d_6) δ 175.80, 173.23, 159.49, 158.61, 151.28, 143.69, 141.90, 139.78, 139.38, 137.51, 131.25, 130.20, 129.79, 128.97, 128.57, 124.62, 123.86, 120.51, 116.74, 115.23, 113.78, 110.47, 85.25, 83.69, 61.52, 37.81, 34.35, 31.60, 29.65, 26.25, 25.54, 20.84; HRMS (ESI) calcd for $C_{32}H_{32}NO_9S$ $[M - H]^-$, 606.1805; found 606.1803.

8-(4-(6-(4-Hydroxyphenoxysulfonyl)-3-(4-hydroxyphenyl)-7-oxabicyclo[2.2.1]hept-2-en-2-yl)phenylamino)-8-oxooctanoic Acid (23h). Pale yellow solid, 83% yield, m.p. 120-121 °C; ^{1}H NMR (400 MHz, Acetone-d_6) δ 9.36 (s, 1H), 7.65 (t, J = 8.4 Hz, 2H), 7.33 (t, J = 8.8 Hz, 2H), 7.28 (t, J = 8.4 Hz, 2H), 7.11 (t, J = 9.2 Hz, 2H), 6.85 (d, J = 8.8 Hz, 1H), 6.84 (m, 3H), 5.69 (s, 1H), 5.46 (s, 1H), 3.81 (m, 1H), 2.40 (m, 3H), 2.30 (t, J = 7.2 Hz, 3H), 1.70 (t, J = 6.4 Hz, 2H), 1.61 (t, J = 6.4 Hz, 2H), 1.37 (m,

4H). ^{13}C NMR (100 MHz, Acetone-d_6) δ 175.44, 172.91, 158.58, 157.08, 143.57, 143.00, 141.87, 139.91, 139.37, 137.57, 130.37, 129.68, 129.13, 128.46, 124.71, 124.23, 120.29, 116.95, 116.68, 116.49, 85.32, 83.68, 61.14, 37.74, 34.27, 31.53, 30.80, 29.57, 26.20, 25.53; HRMS (ESI) calcd for $C_{32}H_{32}NO_9S$ [M - H]$^-$, 606.1805; found 606.1803.

8-(4-(3-(4-Hydroxyphenyl)-6-(2-methoxyphenoxysulfonyl)-7-oxabicyclo[2.2.1]hept-2-en-2-yl)phenylamino)-8-oxooctanoic Acid (23i). Pale yellow solid, 96% yield, m.p. 103-106 °C; ^{1}H NMR (400 MHz, Acetone-d_6) δ 9.31 (s, 1H), 7.67 (t, J = 8.0 Hz, 2H), 7.33 (m, 6H), 7.11 (d, J = 8.0 Hz, 1H), 6.98 (t, J = 8.0 Hz, 1H), 6.82 (t, J = 8.0 Hz, 2H), 5.69 (s, 1H), 5.44 (t, J = 3.2 Hz, 1H), 3.74 (m, 1H), 3.71 (s, 3H, -OMe), 2.51 (m, 1H), 2.41 (t, J = 7.6 Hz, 2H), 2.31 (t, J = 7.6 Hz, 2H), 2.07 (m, 1H), 1.71 (t, J = 6.8 Hz, 2H), 1.61 (t, J = 6.8 Hz, 2H), 1.37 (m, 4H). ^{13}C NMR (100 MHz, Acetone-d_6) δ 175.06, 172.51, 158.62, 158.56, 152.62, 143.73, 142.14, 139.31, 137.69, 130.12, 129.78, 128.95, 128.88, 128.56, 124.74, 124.06, 121.61, 120.35, 120.17, 116.68, 116.53, 114.14, 85.26, 83.61, 62.48, 56.25, 37.72, 34.23, 31.72, 30.70, 29.66, 26.14, 25.54; HRMS (ESI) calcd for $C_{33}H_{34}NO_9S$ [M - H]$^-$, 620.1970 ; found 620.1967.

8-(4-(6-(4-Fluorophenoxysulfonyl)-3-(4-hydroxyphenyl)-7-oxabicyclo[2.2.1]hept-2-en-2-yl)phenylamino)-8-oxooctanoic Acid (23j). Pale yellow solid, 78% yield, m.p. 105-107 °C; ^{1}H NMR (400 MHz, Acetone-d_6) δ 7.56 (t, J = 9.6 Hz, 2H), 7.21 (m, 4H), 7.11 (t, J = 8.4 Hz, 2H), 7.05 (m, 2H), 6.72 (d, J = 8.8 Hz, 1H), 6.96 (d, J = 8.8 Hz, 1H), 5.55 (s, 1H), 5.34 (t, J = 3.2 Hz, 1H), 3.71 (m, 1H), 2.28 (m, 3H), 2.22 (t, J = 7.6 Hz, 2H), 1.95 (m, 1H), 1.55 (t, J = 6.8 Hz, 2H), 1.47 (t, J = 7.6 Hz, 2H), 1.23 (m, 4H). ^{13}C NMR (100 MHz, Acetone-d_6) δ 174.17, 172.19, 163.05, 160.62, 158.51, 146.41, 143.49, 141.95, 140.28, 139.18, 137.54, 130.26, 129.65, 129.05, 128.45, 125.07, 120.20, 119.95, 117.46, 117.22, 116.58, 116.40, 85.22, 83.65, 61.67, 51.52, 37.62, 34.28, 31.54, 31.34, 26.06, 25.52; HRMS (ESI) calcd for $C_{32}H_{31}FNO_8S$ [M - H]$^-$, 608.1762; found 608.1760.

8-(4-(6-(2-Hydroxyphenoxysulfonyl)-3-(4-hydroxyphenyl)-7-oxabicyclo[2.2.1]hept-2-en-2-yl)phenylamino)-8-oxooctanoic Acid (23k). Pale yellow solid, 81% yield, m.p. 116-118 °C; ^{1}H NMR (400 MHz, Acetone-d_6) δ 9.35 (s, 1H), 7.65 (d, J = 8.8 Hz,

2H), 7.32 (m, 5H), 7.13 (t, *J* = 8.4 Hz, 1H), 7.03 (d, *J* = 8.0 Hz, 1H), 6.88 (m, 3H), 5.76 (s, 1H), 5.48 (t, *J* = 4.0 Hz, 1H), 4.02 (m, 1H), 2.51 (m, 1H), 2.40 (t, *J* = 7.6 Hz, 2H), 2.31 (t, *J* = 7.2 Hz, 2H), 2.24 (m, 1H), 1.71 (t, *J* = 6.8 Hz, 2H), 1.61 (t, *J* = 6.8 Hz, 2H), 1.37 (m, 4H). ^{13}C NMR (100 MHz, Acetone-d_6) δ 175.56, 173.04, 158.55, 150.15, 143.67, 141.90, 139.91, 139.38, 138.26, 137.60, 130.03, 129.88, 128.82, 128.66, 124.81, 123.96, 120.87, 1120.47, 118.45, 116.66, 116.57, 85.29, 83.74, 62.55, 37.77, 34.30, 31.46, 29.56, 26.22, 25.53, 20.76; HRMS (ESI) calcd for $C_{32}H_{32}NO_9S$ [M - H]$^-$, 606.1804; found 606.1803.

8-(4-(6-(4-Chlorophenoxysulfonyl)-3-(4-hydroxyphenyl)-7-oxabicyclo[2.2.1]hept-2-en-2-yl)phenylamino)-8-oxooctanoic Acid (23l). Pale yellow solid, 74% yield, m.p. 93-95 °C; ^{1}H NMR (400 MHz, Acetone-d_6) δ 9.33 (s, 1H), 7.65 (t, *J* = 9.2 Hz, 2H), 7.42 (d, *J* = 9.6 Hz, 2H), 7.31 (m, 4H), 7.25 (t, *J* = 7.6 Hz, 2H), 6.86 (d, *J* = 8.0 Hz, 1H), 6.82 (d, *J* = 8.8 Hz, 1H), 5.69 (s, 1H), 5.48 (t, *J* = 3.2 Hz, 1H), 3.89 (m, 1H), 2.39 (m, 3H), 2.31 (t, *J* = 7.6 Hz, 2H), 2.09 (m, 1H), 1.69 (m, 2H), 1.60 (t, *J* = 7.2 Hz, 2H), 1.38 (m, 4H). ^{13}C NMR (100 MHz, Acetone-d_6) δ 175.13, 172.52, 158.47, 149.10, 143.53, 141.95, 140.03, 139.18, 137.49, 133.03, 130.78, 130.29, 129.69, 129.07, 128.48, 124.92, 120.32, 120.11, 116.62, 106.44, 85.21, 83.67, 61.69, 37.70, 34.20, 31.56, 31.35, 26.15, 25.52, 20.63; HRMS (ESI) calcd for $C_{32}H_{31}ClNO_8S$ [M - H]$^-$, 624.1469; found 624.1464.

8-(4-(6-(4-Bromophenoxysulfonyl)-3-(4-hydroxyphenyl)-7-oxabicyclo[2.2.1]hept-2-en-2-yl)phenylamino)-8-oxooctanoic Acid (23m). Pale yellow solid, 72% yield, m.p. 104-107 °C; ^{1}H NMR (400 MHz, Acetone-d_6) δ 9.32 (s, 1H), 7.67 (t, *J* = 9.2 Hz, 2H), 7.57 (d, *J* = 8.4 Hz, 2H), 7.32 (t, *J* = 8.0 Hz, 2H), 7.26 (m, 4H), 6.86 (d, *J* = 8.8 Hz, 1H), 6.82 (d, *J* = 8.8 Hz, 1H), 5.69 (s, 1H), 5.47 (t, *J* = 2.8 Hz, 1H), 3.86 (m, 1H), 2.45 (m, 3H), 2.31 (t, *J* = 7.2 Hz, 2H), 2.06 (m, 1H), 1.70 (m, 2H), 1.60 (t, *J* = 6.8 Hz, 2H), 1.37 (m, 4H). ^{13}C NMR (100 MHz, Acetone-d_6) δ 175.49, 172.31, 158.50, 149.67, 143.51, 141.96, 140.13, 139.16, 137.50, 133.83, 130.27, 129.67, 129.07, 128.47, 125.26, 124.62, 123.84, 120.81, 120.24, 120.02, 116.60, 116.42, 85.21, 83.70, 61.87, 37.67, 34.18, 31.55, 31.35, 29.65, 26.13, 25.52; HRMS (ESI) calcd for $C_{32}H_{31}BrNO_8S$ [M - H]$^-$, 668.0961; found 668.0959.

8-(4-(3-(4-Hydroxyphenyl)-6-(4-(trifluoromethyl)phenoxysulfonyl)-7-oxabicyclo[2.2.1]hept-2-en-2-yl)phenylamino)-8-oxooctanoic Acid (23n). Pale yellow solid, 82% yield, m.p 87-89 °C; ^{1}H NMR (400 MHz, Acetone-d_6) δ 9.33 (s, 1H), 7.79 (d, J = 8.0 Hz, 2H), 7.67 (t, J = 7.6 Hz, 2H), 7.55 (t, J = 8.8 Hz, 2H), 7.34 (t, J = 8.8 Hz, 2H), 7.25 (t, J = 7.6 Hz, 2H), 6.85 (t, J = 8.4 Hz, 2H), 5.73 (s, 1H), 5.50 (t, J = 3.2 Hz, 1H), 3.97 (m, 1H), 2.47 (m, 1H), 2.39 (t, J = 6.8 Hz, 2H), 2.31 (t, J = 7.6 Hz, 2H), 2.05 (m, 1H), 1.70 (t, J = 6.4 Hz, 2H), 1.62 (t, J = 6.8 Hz, 2H), 1.38 (m, 4H). ^{13}C NMR (100 MHz, Acetone-d_6) δ 175.93, 172.42, 158.49, 153.12, 143.57, 142.00, 140.20, 139.13, 137.47, 130.26, 129.71, 129.04, 128.50, 128.23, 128.20, 126.21, 124.60, 124.01, 123.83, 120.24, 120.04, 116.57, 116.41, 85.18, 83.73, 62.28, 37.66, 34.14, 31.55, 31.34, 29.65, 26.13, 25.50; HRMS (ESI) calcd for $C_{33}H_{31}F_3NO_8S$ [M - H]$^-$, 658.1730; found 658.1728.

8-(4-(3-(4-Hydroxyphenyl)-6-(2-(trifluoromethyl)phenoxysulfonyl)-7-oxabicyclo[2.2.1]hept-2-en-2-yl)phenylamino)-8-oxooctanoic Acid (23o). Pale yellow solid, 80% yield, m.p 91-92 °C; ^{1}H NMR (400 MHz, Acetone-d_6) δ 9.33 (s, 1H), 7.84 (d, J = 8.0 Hz, 1H), 7.77 (t, J = 7.6 Hz, 2H), 7.68 (d, J = 8.4 Hz, 2H), 7.56 (t, J = 7.2 Hz, 1H), 7.30 (m, 2H), 7.14 (m, 2H), 6.85 (d, J = 8.4 Hz, 2H), 5.78 (s, 1H), 5.53 (t, J = 3.6 Hz, 1H), 4.02 (m, 1H), 2.56 (m, 1H), 2.41 (m, 3H), 2.31 (t, J = 7.6 Hz, 2H), 1.71 (t, J = 6.8 Hz, 2H), 1.62 (t, J = 7.2 Hz, 2H), 1.38 (m, 4H). ^{13}C NMR (100 MHz, Acetone-d_6) δ 175.12, 172.52, 158.54, 147.63, 143.74, 142.19, 140.20, 139.20, 137.44, 135.13, 131.68, 129.93, 129.88, 128.73, 128.69, 128.62, 127.83, 124.52, 123.74, 120.17, 120.10, 116.54, 116.47, 85.08, 83.70, 63.14, 37.68, 34.19, 31.20, 30.13, 26.14, 25.51, 20.59; HRMS (ESI) calcd for $C_{33}H_{31}F_3NO_8S$ [M - H]$^-$, 658.1730; found 658.1728.

8-(4-(6-(2,6-Dimethylphenoxysulfonyl)-3-(4-hydroxyphenyl)-7-oxabicyclo[2.2.1]hept-2-en-2-yl)phenylamino)-8-oxooctanoic Acid (23p). Pale yellow solid, 93% yield m.p. 106-107 °C; ^{1}H NMR (400 MHz, Acetone-d_6) δ 9.33 (s, 1H), 7.69 (t, J = 8.0 Hz, 2H), 7.38 (d, J = 8.8 Hz, 1H), 7.34 (d, J = 9.2 Hz, 1H), 7.30 (t, J = 8.4 Hz, 2H), 7.10 (m, 3H), 6.86 (t, J = 8.4 Hz, 2H), 5.81 (s, 1H), 5.51 (t, J = 3.6 Hz, 1H), 4.01 (m, 1H), 2.64 (m, 1H), 2.44 (t, J = 7.6 Hz, 2H), 2.34 (s, 3H), 2.31 (s, 3H), 2.29 (t, J = 7.2 Hz, 2H), 2.04 (m, 1H), 1.69 (m, 2H), 1.61 (t, J = 6.0 Hz, 2H), 1.37 (m, 4H). ^{13}C NMR

(100 MHz, Acetone-d_6) δ 175.26, 172.57, 158.61, 147.45, 143.68, 142.04, 140.23, 139.37, 137.68, 133.25, 130.18, 130.15, 129.80, 128.91, 128.58, 127.71, 124.70, 123.97, 120.34, 120.21, 116.69, 116.54, 85.37, 83.79, 62.91, 37.74, 34.28, 31.71, 31.49, 29.66, 26.16, 25.54, 17.90, 17.88; HRMS (ESI) calcd for $C_{34}H_{36}NO_8S$ $[M - H]^-$, 618.2171; found 618.2167.

8-(4-(3-(4-Hydroxyphenyl)-6-(naphthalen-2-yloxysulfonyl)-7-oxabicyclo[2.2.1]hept-2-en-2-yl)phenylamino)-8-oxooctanoic Acid (23q). Pale yellow solid, 90% yield, m.p. 86-88 °C; ^{1}H NMR (400 MHz, CD_3OD) δ 7.99 (m, 1H), 7.89 (m, 1H), 7.79 (d, J = 8.0 Hz, 1H), 7.56 (m, 3H), 7.45 (m, 3H), 7.33 (m, 3H), 7.24 (d, J = 8.8 Hz, 1H), 6.74 (d, J = 8.4 Hz, 1H), 6.65 (d, J = 8.8 Hz, 1H), 5.71 (s, 1H), 5.35 (s, 1H), 4.49 (m, 1H), 2.63 (m, 1H), 2.37 (t, J = 6.0 Hz, 2H), 2.30 (t, J = 6.4 Hz, 2H), 2.06 (m, 1H), 1.69 (m, 2H), 1.60 (t, J = 6.4 Hz, 2H), 1.38 (m, 4H). ^{13}C NMR (100 MHz, CD_3OD) δ 176.20, 173.22, 157.55, 157.07, 144.63, 142.76, 140.37, 138.24, 137.76, 135.43, 134.83, 129.46, 129.07, 128.25, 127.89, 127.19, 126.80, 126.53, 124.94, 123.62, 121.39, 119.75, 119.13, 118.28, 115.17, 114.57, 84.27, 82.93, 60.11, 36.48, 33.42, 29.41, 28.55, 28.50, 25.34, 24.49; HRMS (ESI) calcd for $C_{36}H_{34}NO_8S$ $[M - H]^-$, 640.2013; found 640.2011.

8-(4-(3-(4-Hydroxyphenyl)-6-(naphthalen-2-yloxysulfonyl)-7-oxabicyclo[2.2.1]hept-2-en-2-yl)phenylamino)-8-oxooctanoic Acid (23r). White solid, 94% yield, m.p. 93-96 °C; ^{1}H NMR (400 MHz, CD_3OD) δ 7.85 (m, 2H), 7.69 (t, J = 9.2 Hz, 1H), 7.59 (d, J = 8.8 Hz, 1H), 7.51 (m, 4H), 7.34 (m, 1H), 7.26 (t, J = 8.4 Hz, 2H), 7.18 (t, J = 8.0 Hz, 1H), 7.15 (d, J = 8.4 Hz, 1H), 6.76 (d, J = 7.6 Hz, 1H), 6.69 (d, J = 8.0 Hz, 1H), 5.70 (s, 1H), 5.39 (t, J = 4.0 Hz, 1H), 3.80 (m, 1H), 2.48 (m, 1H), 2.40 (m, 2H), 2.23 (m, 2H), 1.68 (t, J = 7.2 Hz, 2H), 1.60 (m, 2H), 1.38 (m, 4H). ^{13}C NMR (100 MHz, CD_3OD) δ 173.30, 173.26, 157.86, 157.55, 147.00, 142.77, 140.65, 138.57, 138.36, 136.05, 133.48, 131.90, 129.74, 129.20, 128.35, 127.99, 127.14, 126.67, 126.17, 123.26, 122.47, 120.72, 119.98, 119.10, 115.52, 115.16, 84.35, 82.65, 59.81, 36.54, 34.94, 29.92, 28.68, 28.63, 25.39, 25.07; HRMS (ESI) calcd for $C_{36}H_{34}NO_8S$ $(M - H)^-$, 640.2013; found 640.2011.

6-(4-(8-(Hydroxyamino)-8-oxooctanamido)phenyl)-5-(4-hydroxyphenyl)-7-oxabic

yclo[2.2.1]hept-5-ene-2-sulfonic Acid 2-Phenyl Este (24a). Pale yellow solid, 76% yield, m.p. 93-95 °C; ^{1}H NMR (400 MHz, Acetone-d_6) δ 9.64 (s, 1H), 7.70 (m, 1H), 7.38 (d, J = 8.0 Hz, 2H), 7.32 (d, J = 7.2 Hz, 1H), 7.27 (d, J = 7.6 Hz, 4H), 7.34 (d, J = 8.4 Hz, 3H), 6.86 (m, 1H), 5.68 (s, 1H), 5.47 (s, 1H), 3.75 (m, 1H), 2.41 (m, 3H), 2.24 (m, 1H), 2.13 (t, J = 6.8 Hz, 2H), 1.60 (m, 4H), 1.35 (m, 4H). ^{13}C NMR (100 MHz, Acetone-d_6) δ 172.40, 171.26, 158.83, 158.72, 150.53, 138.62, 137.55, 130.85, 130.83, 130.22, 129.60, 128.97, 128.37, 128.03, 127.88, 124.52, 123.18, 123.16, 120.37, 120.27, 116.72, 116.53, 85.21, 83.54, 61.63, 46.83, 37.63, 33.20, 31.34, 26.12, 26.10, 20.69; HRMS (ESI) calcd for $C_{32}H_{35}N_2O_8S$ $[M + H]^+$, 607.2114; found 607.2114.

6-(4-(8-(Hydroxyamino)-8-oxooctanamido)phenyl)-5-(4-hydroxyphenyl)-7-oxabic yclo[2.2.1]hept-5-ene-2-sulfonic Acid 4-Tolyl Este (24b). Pale yellow solid, 83% yield, m.p. 97-100 °C; ^{1}H NMR (400 MHz, Acetone-d_6) δ 7.65 (d, J = 8.0 Hz, 1H), 7.24 (d, J = 8.8 Hz, 4H), 7.11 (m, 6H), 6.83 (d, J = 7.2 Hz, 1H), 5.67 (s, 1H), 5.46 (s, 1H), 3.73 (m, 1H), 2.41 (m, 3H), 2.30 (s, 3H, -Me), 2.15 (m, 3H), 1.63 (t, J = 6.8 Hz, 4H), 1.35 (m, 4H). ^{13}C NMR (100 MHz, Acetone-d_6) δ 172.52, 171.77, 158.61, 158.47, 148.38, 143.49, 141.81, 139.27, 137.83, 137.57, 131.21, 130.30, 129.65, 129.07, 128.43, 124.66, 123.87, 122.86, 122.83, 120.28, 116.61, 116.42, 85.23, 83.62, 61.18, 37.66, 31.53, 31.34, 26.11, 26.04, 20.87, 20.85; HRMS (ESI) calcd for $C_{33}H_{37}N_2O_8S$ $[M + H]^+$, 621.2271; found 621.2272.

6-(4-(8-(Hydroxyamino)-8-oxooctanamido)phenyl)-5-(4-hydroxyphenyl)-7-oxabic yclo[2.2.1]hept-5-ene-2-sulfonic Acid 3-Tolyl Este (24c). Pale yellow solid, 79% yield, m.p. 92-94 °C; ^{1}H NMR (400 MHz, Acetone-d_6) δ 9.84 (s, 1H), 7.69 (d, J = 8.8 Hz, 2H), 7.22 (m, 5H), 7.12 (d, J = 7.2 Hz, 1H), 7.03 (t, J = 8.4 Hz, 2H), 6.88 (t, J = 8.0 Hz, 2H), 5.68 (s, 1H), 5.46 (s, 1H), 3.73 (m, 1H), 2.42 (m, 3H), 2.29 (m, 1H), 2.27 (s, 3H, -Me), 2.13 (t, J = 7.6 Hz, 2H), 1.60 (m, 4H), 1.34 (m, 4H). ^{13}C NMR (100 MHz, Acetone-d_6) δ 172.76, 171.53, 158.80, 150.46, 143.53, 141.87, 141.22, 140.46, 139.22, 137.43, 130.53, 130.25, 129.55, 129.00, 128.73, 128.31, 124.47, 123.50, 120.44, 120.09, 116.81, 116.58, 85.19, 83.66, 61.45, 46.94, 37.65, 33.24, 31.49, 31.30, 26.18, 21.27, 20.82; HRMS (ESI) calcd for $C_{33}H_{37}N_2O_8S$ $[M + H]^+$, 621.2271; found

621.2272.

6-(4-(8-(Hydroxyamino)-8-oxooctanamido)phenyl)-5-(4-hydroxyphenyl)-7-oxabicyclo[2.2.1]hept-5-ene-2-sulfonic Acid 2-Tolyl Este (24d). Pale yellow solid, 76% yield, m.p. 89-91 °C; ^{1}H NMR (400 MHz, Acetone-d_6) δ 9.48 (s, 1H), 7.68 (m, 2H), 7.27 (m, 6H), 7.19 (t, J = 8.0 Hz, 2H), 6.84 (m, 2H), 5.72 (s, 1H), 5.49 (d, J = 3.6 Hz, 1H), 3.89 (m, 1H), 2.51 (m, 1H), 2.36 (t, J = 7.6 Hz, 3H), 2.15 (m, 2H), 1.61 (m, 4H), 1.34 (m, 4H). ^{13}C NMR (100 MHz, Acetone-d_6) δ 171.77, 170.70, 157.72, 147.96, 142.75, 141.06, 139.20, 138.43, 136.68, 131.75, 129.26, 128.88, 128.10, 127.65, 127.21, 127.00, 123.69, 122.95, 122.18, 119.44, 115.78, 115.62, 84.35, 82.87, 61.54, 36.77, 32.36, 30.50, 29.58, 25.23, 16.04; HRMS (ESI) calcd for $C_{33}H_{37}N_2O_8S$ [M + H]$^+$, 621.2271; found 621.2274.

6-(4-(8-(Hydroxyamino)-8-oxooctanamido)phenyl)-5-(4-hydroxyphenyl)-7-oxabicyclo[2.2.1]hept-5-ene-2-sulfonic Acid 2-Methoxyphenyl Este (24e). Pale yellow solid, 87% yield, m.p. 96-99 °C; ^{1}H NMR (400 MHz, Acetone-d_6) δ 9.65 (s, 1H), 7.72 (m, 2H), 7.24 (m, 6H), 7.10 (d, J = 8.4 Hz, 1H), 6.94 (t, J = 7.6 Hz, 1H), 6.86 (m, 2H), 5.68 (s, 1H), 5.44 (d, J = 4.0 Hz, 1H), 3.86 (m, 1H), 3.72 (s, 3H, -OMe), 2.40 (m, 3H), 2.27 (m, 1H), 2.12 (t, J = 6.4 Hz, 2H), 1.60 (m, 4H), 1.34 (m, 4H). ^{13}C NMR (100 MHz, Acetone-d_6) δ 172.48, 171.25, 158.72, 152.70, 143.68, 142.11, 139.30, 137.63, 130.05, 129.70, 128.96, 128.79, 128.47, 128.02, 124.69, 124.57, 123.89, 121.60, 120.26, 116.65, 116.54, 114.17, 85.25, 83.63, 62.59, 56.26, 46.80, 37.57, 33.21, 31.73, 31.48, 26.08, 20.73; HRMS (ESI) calcd for $C_{33}H_{37}N_2O_9S$ [M + H]$^+$, 637.2202; found 637.2206.

6-(4-(8-(Hydroxyamino)-8-oxooctanamido)phenyl)-5-(4-hydroxyphenyl)-7-oxabicyclo[2.2.1]hept-5-ene-2-sulfonic Acid 4-Fluorophenyl Este (24f). Pale yellow solid, 73% yield, m.p. 101-103 °C; ^{1}H NMR (400 MHz, Acetone-d_6) δ 9.78 (s, 1H), 7.73 (m, 2H), 7.30 (d, J = 7.6 Hz, 4H), 7.20 (d, J = 8.0 Hz, 2H), 7.14 (m, 2H), 6.87 (m, 2H), 5.69 (s, 1H), 5.48 (s, 1H), 3.78 (m, 1H), 2.40 (t, J = 6.0 Hz, 3H), 2.28 (m, 1H), 2.13 (t, J = 7.2 Hz, 2H), 1.60 (m, 4H), 1.34 (m, 4H). ^{13}C NMR (100 MHz, Acetone-d_6) δ 172.75, 171.50, 163.04, 160.61, 158.84, 146.36, 143.53, 141.87, 140.41, 139.16, 137.40, 130.20, 129.61, 128.95, 128.36, 125.20, 123.63, 120.47, 117.51, 117.27,

116.77, 116.59, 85.20, 83.70, 61.71, 46.97, 37.64, 33.23, 31.57, 31.36, 26.16, 20.80; HRMS (ESI) calcd for $C_{32}H_{34}FN_2O_8S$ $[M + H]^+$, 625.2002; found 625.2005.

6-(4-(8-(Hydroxyamino)-8-oxooctanamido)phenyl)-5-(4-hydroxyphenyl)-7-oxabicyclo[2.2.1]hept-5-ene-2-sulfonic Acid 4-Bromophenyl Este (24g). Pale yellow solid, 70% yield, m.p. 111-113 °C; ^{1}H NMR (400 MHz, Acetone-d_6) δ 9.40 (s, 1H), 7.66 (m, 2H), 7.55 (d, J = 8.0 Hz, 2H), 7.30 (m, 2H), 7.24 (d, J = 8.8 Hz, 4H), 6.84 (d, J = 7.2 Hz, 2H), 5.69 (s, 1H), 5.48 (s, 1H), 3.82 (m, 1H), 2.40 (t, J = 7.6 Hz, 3H), 2.28 (m, 1H), 2.13 (t, J = 7.6 Hz, 2H), 1.61 (m, 4H), 1.35 (m, 4H). ^{13}C NMR (100 MHz, Acetone-d_6) δ 172.71, 171.44, 158.61, 149.63, 143.54, 141.91, 140.26, 139.18, 137.44, 133.84, 133.83, 130.28, 129.67, 129.06, 128.45, 125.31, 124.55, 123.77, 120.83, 120.41, 116.68, 116.50, 85.20, 83.71, 61.86, 37.69, 33.22, 31.55, 31.35, 26.14, 26.12, 20.69; HRMS (ESI) calcd for $C_{32}H_{34}BrN_2O_8S$ $[M + H]^+$, 685.1210; found 685.1208.

6-(4-(8-(Hydroxyamino)-8-oxooctanamido)phenyl)-5-(4-hydroxyphenyl)-7-oxabicyclo[2.2.1]hept-5-ene-2-sulfonic Acid 1-Naphthalen Este (24h). Pale yellow solid, 88% yield, m.p. 106-109 °C; ^{1}H NMR (400 MHz, Acetone-d_6) δ 9.24 (s, 1H), 7.79 (d, J = 8.0 Hz, 2H), 7.68 (m, 1H), 7.51 (t, J = 8.8 Hz, 3H), 7.40 (d, J = 7.2 Hz, 2H), 7.28 (d, J = 8.0 Hz, 1H), 7.10 (t, J = 7.6 Hz, 4H), 6.68 (d, J = 8.4 Hz, 2H), 5.62 (s, 1H), 5.34 (s, 1H), 3.78 (m, 1H), 2.23 (m, 4H), 1.99 (m, 2H), 1.46 (m, 4H), 1.21 (m, 4H). ^{13}C NMR (100 MHz, Acetone-d_6) δ 172.39, 171.20, 158.71, 158.52, 148.25, 143.51, 141.96, 139.23, 137.55, 134.51, 132.85, 130.96, 130.36, 129.59, 129.20, 128.78, 128.67, 128.41, 127.93, 127.38, 124.71, 123.87, 122.25, 120.40, 116.70, 116.45, 85.21, 83.69, 61.46, 37.69, 33.20, 31.52, 31.31, 26.14, 26.09, 20.60; HRMS (ESI) calcd for $C_{36}H_{37}N_2O_8S$ $[M + H]^+$, 657.2261; found 657.2256.

6-(4-(8-(Hydroxyamino)-8-oxooctanamido)phenyl)-5-(4-hydroxyphenyl)-7-oxabicyclo[2.2.1]hept-5-ene-2-sulfonic Acid 2-Naphthalen Este (24i). Pale yellow solid, 85% yield, m.p. 85-87 °C; ^{1}H NMR (400 MHz, Acetone-d_6) δ 9.80 (s, 1H), 7.93 (d, J = 8.4 Hz, 2H), 7.71 (m, 4H), 7.52 (d, J = 8.8 Hz, 2H), 7.42 (d, J = 8.8 Hz, 1H), 7.31 (d, J = 7.2 Hz, 1H), 7.26 (m, 3H), 6.87 (m, 2H), 5.75 (s, 1H), 5.47 (s, 1H), 3.97 (m, 1H), 3.18 (m, 1H), 2.44 (m, 4H), 2.15 (m, 1H), 1.65 (m, 4H), 1.31 (m, 4H). ^{13}C NMR (100 MHz, Acetone-d_6) δ 172.84, 171.60, 158.96, 158.77, 148.11, 143.54, 141.91,

139.20, 137.44, 134.50, 132.84, 131.01, 130.29, 129.53, 129.11, 128.81, 128.69, 128.33, 127.99, 127.41, 124.49, 123.67, 122.25, 120.42, 116.83, 116.59, 85.29, 83.67, 61.40, 46.94, 37.64, 33.29, 31.56, 31.32, 26.14, 9.10; HRMS (ESI) calcd for $C_{36}H_{36}ClN_2O_8S$ $[M + Cl]^-$, 691.1919; found 691.1916.

Estrogen Receptor Binding Affinity. Relative binding affinities were determined by a competitive fluorometric binding assay as previously described. Briefly, 40 nM fluorescence tracer (coumestrol, Sigma-Aldrich, MO) and 0.8 μM purified human ERα or ERβ ligand binding domain (LBD) were diluted in 100 mM potassium phosphate buffer (pH 7.4), containing 100 μg/mL bovine gamma globulin (Sigma-Aldrich, MO), and an equal volume of tested compound was added. Incubations were for 2h at room temperature (25 °C). Fluorescence polarization values were then measured. The binding affinities are expressed as relative binding affinity (RBA) values with the RBA of 17-β estradiol set to 100%. The values given are the average ± range of two independent determinations. IC_{50} values were calculated according to equations described previously.[19]

Gene Transcriptional Activity. The human embryonic kidney cell lines, HEK 293T, was maintained in Dulbecco's Minimum Essential Medium (DMEM) (Gibco by Invitrogen Corp., CA) with 10% fetal bovine serum (FBS) (Hylcone by Thermo Scientific, UT). Cells were plated in phenol red-free DMEM with 10% FBS. HEK 293T cells were transfected with 25 μL mixture per well, containing 300 ng of 3 × ERE-luciferase reporter, 100 ng of ERα or ERβ expression vector, 125 mM calcium chloride (GuoYao, China) and 12.5 μL 2 × HBS. The next day, the cells were treated with increasing doses of ER ligands diluted in phenol red-free DMEM with 10% FBS. After 24h, luciferase activity was measured using Dual-Luciferase Reporter Assay System (Promega, MI) according to the manufacturer's protocol.

Cell Culture and Cell Viability Assay. The human breast cancer cell lines MCF-7 was obtained from ATCC. DU145 and VERO cells were obtained from cell bank of Chinese Academy of Science (Shanghai, China). Cells were maintained in DMEM with 10% FBS. For all experiments, cells were grown in 96-well microtiter plates (Nest Biotech Co., China) with appropriate ligand triplicate for 72h. MTT colormetric

tests (Biosharp, China) were employed to determine cell viability per manufacturer instructions. IC_{50} values were calculated according to the following equation using Origin software: Y = 100% inhibition + (0% inhibition - 100% inhibition)/(1 + $10^{[(LogIC50-X)\times Hillslope]}$), where Y = fluorescence value, X = Log [inhibitor].[19]

HDAC Activity Assay. *In vitro* HDAC activity was measured using Fluorogenic HDAC1/HDAC6 Assay Kit (BPS Bioscience, CA) according to the manufacturer's protocol. All of the tested compounds were prepared in DMSO and were diluted in HDAC assay buffer to different concentration. The enzymatic reactions were conducted in duplicate at 37 ℃ for 30 min in a 50 μL mixture containing HDAC assay buffer, 5 μg of BSA, HDAC substrate, HDAC enzyme (human recombinant HDAC1, HDAC6), and various concentrations of tested compound. Then, 50 μL of 2 × HDAC Developer was added to each well and the plate was incubated at room temperature for 15 min. Fluorescence values were measured at an excitation of 350 nm and an emission of 440 nm using SpectraMax M2 microplate reader. IC_{50} values were calculated according to the following equation using Origin software: $Y = F_b + (F_t-F_b)/(1+10^{[(LogIC50-X)\times Hillslope]})$, where Y = fluorescence value, F_b = minimum fluorescence value, F_t = maximum fluorescence value, X = Log [inhibitor].

Molecular Modeling. Crystal structures of ER LBD in complex with 4-hydroxytamoxifen was downloaded from the protein data bank (PDB ID: 3ERT). Compounds **21a**, and **23q** were docked into the three-dimension structure of ERα LBD with AutoDock software (version 4.2).[44, 45] Crystallographic coordinates of the **21a**, and **23q** were created by Biochemoffice. The crystal structure of ERα LBD (PDB ID: 3ERD)[39] was obtained from the PDB and all water molecules were removed. Preparations of all ligands and the protein were performed with AutoDockTools (ADT). A docking cube with the edge of 60 Å, 60 Å, 58 Å in X, Y, Z dimension respectively (a grid spacing of 0.375 Å), which encompassed the whole active site, was used throughout docking. On the basis of the Lamarckian genetic algorithm (LGA), 80 runs were performed for each ligand with 500 individuals in the population.[38] The figures were prepared using PyMOL.

Acknowledgments

We are grateful to the NSFC (81172935, 81373255, 31371331), Key Project of Ministry of Education (313040), Hubei Province's Outstanding Medical Academic Leader Program, and the Fundamental Research Funds for the Central Universities (2014306020201 and 2042014kf0204) for support of this research. Prof. John A. Katzenellenbogen is thanked for critical reading of this manuscript.

Supporting Information:

Synthetic procedures and characterization data for compounds **6**, **8-12**, **14-16**, and **19**; ^{1}H NMR and ^{13}C NMR spectral information, and HPLC results and HPLC spectra for compounds **20-24**. This material is available free of charge via the Internet at http://pubs.acs.org.

Corresponding Author Information

Hai-Bing Zhou, Tel 86 27 68759586, zhouhb@whu.edu.cn;

Chun Dong, Tel 86 27 68759586, cdong@whu.edu.cn;

Jian Huang, Tel 86 27 68753582, jianhuang@whu.edu.cn.

ABBREVIATIONS USED

E_2, estradiol; ER, estrogen receptor; AF2, transcriptional activation function 2; HDAC, histone deacetylases; HDACi, histone deacetylase inhibitor; SERMs, selective estrogen receptor modulators; RBA, relative binding affinity; SAHA, suberoylanilide hydroxamic acid; LBD, ligand binding domain; NBS, *N*-bromosuccinimide; THF, tetrahydrofuran; TLC, thin layer chromatography; OBHS, *exo*-5,6-bis-(4-hydroxyphenyl)-7-oxabicyclo[2.2.1]hept-5-ene-2-sulfonic acid phenyl ester; ERE, estrogen response element; DMEM, Dulbecco's minimum essential medium; FBS, fetal bovine serum.

References

(1) Anders, C. K.; Johnson, R.; Litton, J.; Phillips, M.; Bleyer, A. Breast cancer

before age 40 years. *Semin. Oncol.* **2009**, *36*, 237-249.

(2) Jordan, V. C. Antiestrogens and selective estrogen receptor modulators as multifunctional medicines. 1. Receptor interactions. *J. Med. Chem.* **2003**, *46*, 883-908.

(3) Jordan, V. C. Antiestrogens and selective estrogen receptor modulators as multifunctional medicines. 2. Clinical considerations and new agents. *J. Med. Chem.* **2003**, *46*, 1081-1111.

(4) Katzenellenbogen, B. S.; Katzenellenbogen, J. A. Biomedicine. Defining the "S" in SERMs. *Science* **2002**, *295*, 2380-2381.

(5) Shang, Y.; Brown, M. Molecular determinants for the tissue specificity of SERMs. *Science* **2002**, *295*, 2465-2468.

(6) Jordan, V. C. Tamoxifen: a most unlikely pioneering medicine. *Nat. Rev. Drug. Discovery* **2003**, *2*, 205-213.

(7) Ariazi, E. A.; Ariazi, J. L.; Cordera, F.; Jordan, V. C. Estrogen receptors as therapeutic targets in breast cancer. *Curr. Top. Med. Chem.* **2006**, *6*, 181-202.

(8) Clarke, R.; Liu, M. C.; Bouker, K. B.; Gu , Z.; Lee, R. Y.; Zhu, Y.; Skaar, T. C.; Gomez, B.; O'Brien, K.; Wang, Y.; Hilakivi-Clarke, L. A. Antiestrogen resistance in breast cancer and the role of estrogen receptor signaling. *Oncogene* **2003**, *22*, 7316-7339.

(9) Irvin, W. J. Jr.; Carey, L. A. What is triple-negative breast cancer? *Eur. J. Cancer* **2008**, *44*, 2799-2805.

(10) van Leeuwen, F. E.; Benraadt, J.; Coebergh, J. W.; Kiemeney, L. A.; Gimbrere, C. H.; Otter, R.; Schouten, L. J.; Damhuis, R. A.; Bontenbal, M.; Diepenhorst, F. W. Risk of endometrial cancer after tamoxifen treatment of breast cancer. *Lancet* **1994**, *343*, 448-452.

(11) Lv, W.; Liu, J.; Skaar, T. C.; Flockhart, D. A.; Cushman, M. Design and synthesis of norendoxifen analogues with dual aromatase inhibitory and estrogen receptor modulatory activities. *J. Med. Chem.* **2015**, *58*, 2623-2648.

(12) Dao, K. L.; Hanson, R. N. Targeting the estrogen receptor using steroid-therapeutic drug conjugates (hybrids). *Bioconjugate Chem.* **2012**, *23*,

2139-2158.

(13) Devraj, R.; Barrett, J. F.; Fernandez, J. A.; Katzenellenbogen, J. A.; Cushman, M. Design, synthesis, and biological evaluation of ellipticine-estradiol conjugates. *J. Med. Chem.* **1996**, *39*, 3367-3374.

(14) Sharma, U.; Marquis, J. C.; Nicole Dinaut, A.; Hillier, S. M.; Fedeles, B.; Rye, P. T.; Essigmann, J. M.; Croy, R. G. Design, synthesis, and evaluation of estradiol-linked genotoxicants as anti-cancer agents. *Bioorg. Med. Chem. Lett.* **2004**, *14*, 3829-3833.

(15) Burke, P. J.; Koch, T. H. Design, synthesis, and biological evaluation of doxorubicin-formaldehyde conjugates targeted to breast cancer cells. *J. Med. Chem.* **2004**, *47*, 1193-1206.

(16) Zhou, H. B.; Comninos, J. S.; Stossi, F.; Katzenellenbogen, B. S.; Katzenellenbogen, J. A. Synthesis and evaluation of estrogen receptor ligands with bridged oxabicyclic cores containing a diarylethylene motif: estrogen antagonists of unusual structure. *J. Med. Chem.* **2005**, *48*, 7261-7274.

(17) Min, J.; Wang, P.; Srinivasan, S.; Nwachukwu, J. C.; Guo, P.; Huang, M. J.; Carlson, K. E.; Katzenellenbogen, J. A.; Nettles, K. W.; Zhou, H. B. Thiophene-core estrogen receptor ligands having superagonist activity. *J. Med. Chem.* **2013**, *56*, 3346-3366.

(18) Liao, Z. Q.; Dong, C.; Carlson, K. E.; Srinivasan, S.; Nwachukwu, J. C.; Chesnut, R. W.; Sharma, A.; Nettles, K. W.; Katzenellenbogen, J. A.; Zhou, H. B. Triaryl-substituted Schiff bases are high-affinity subtype-selective ligands for the estrogen receptor. *J. Med. Chem.* **2014**, *57*, 3532-3545.

(19) Zheng, Y. F.; Wang, C. H.; Li, C. H.; Qiao, J. X.; Zhang, F.; Huang, M. J.; Ren, W. M.; Dong, C.; Huang, J.; Zhou, H. B. Discovery of novel SERMs with a ferrocenyl entity based on the oxabicyclo[2.2.1]heptene scaffold and evaluation of their antiproliferative effects in breast cancer cells. *Org. Biomol. Chem.* **2012**, *10*, 9689-9699.

(20) Munster, P. N.; Marchion, D.; Thomas, S.; Egorin, M.; Minton, S.; Springett, G.; Lee, J. H.; Simon, G.; Chiappori, A.; Sullivan, D.; Daud, A. Phase I trial of vorinostat and doxorubicin in solid tumours: histone deacetylase 2 expression as a predictive

marker. *Br. J. Cancer* **2009**, *101*, 1044-1050.

(21) Kawai, H.; Li, H.; Avraham, S.; Jiang, S.; Avraham, H. K. Overexpression of histone deacetylase HDAC1 modulates breast cancer progression by negative regulation of estrogen receptor alpha. *Int. J. Cancer* **2003**, *107*, 353-358.

(22) Hodges-Gallagher, L.; Valentine, C. D.; Bader, S. E.; Kushner, P. J. Inhibition of histone deacetylase enhances the anti-proliferative action of antiestrogens on breast cancer cells and blocks tamoxifen-induced proliferation of uterine cells. *Breast. Cancer Res. Treat*. **2007**, *105*, 297-305.

(23) Bicaku, E.; Marchion, D. C.; Schmitt, M. L.; Munster, P. N. Selective inhibition of histone deacetylase 2 silences progesterone receptor-mediated signaling. *Cancer Res*. **2008**, *68*, 1513-1519.

(24) Margueron, R.; Duong, V.; Bonnet, S.; Escande, A.; Vignon, F.; Balaguer, P.; Cavailles, V. Histone deacetylase inhibition and estrogen receptor alpha levels modulate the transcriptional activity of partial antiestrogens. *J. Mol. Endocrinol.* **2004**, *32*, 583-594.

(25) Reid, G.; Metivier, R.; Lin, C. Y.; Denger, S.; Ibberson, D.; Ivacevic, T.; Brand, H.; Benes, V.; Liu, E. T.; Gannon, F. Multiple mechanisms induce transcriptional silencing of a subset of genes, including oestrogen receptor alpha, in response to deacetylase inhibition by valproic acid and trichostatin A. *Oncogene* **2005**, *24*, 4894-4907.

(26) Patel, H. K.; Siklos, M. I.; Abdelkarim, H.; Mendonca, E. L.; Vaidya, A.; Petukhov, P. A.; Thatcher, G. R. A chimeric SERM-histone deacetylase inhibitor approach to breast cancer therapy. *ChemMedChem* **2014**, *9*, 602-613.

(27) Rao, R.; Balusu, R.; Fiskus, W.; Mudunuru, U.; Venkannagari, S.; Chauhan, L.; Smith, J. E.; Hembruff, S. L.; Ha, K.; Atadja, P.; Bhalla, K. N. Combination of pan-histone deacetylase inhibitor and autophagy inhibitor exerts superior efficacy against triple-negative human breast cancer cells. *Mol. Cancer Ther.* **2012**, *11*, 973-983.

(28) Oger, F.; Lecorgne, A.; Sala, E.; Nardese, V.; Demay, F.; Chevance, S.; Desravines, D. C.; Aleksandrova, N.; Guével, R. L.; Lorenzi, S.; Beccari, A. R.;

Barath, P.; Hart, D. J.; Bondon, A.; Carettoni, D.; Simonneaux, G.; Salbert, G. Biological and biophysical properties of the histone deacetylase inhibitor suberoylanilide hydroxamic acid are affected by the presence of short alkyl groups on the phenyl ring. *J. Med. Chem.* **2010**, *53*, 1937-1950.

(29) He, R.; Chen, Y. F.; Chen, Y. H.; Ougolkov, A. V.; Zhang, J. S.; Savoy, D. N.; Billadeau, D. D.; Kozikowski, A. P. Synthesis and biological evaluation of triazol-4-ylphenyl-bearing histone deacetylase inhibitors as anticancer agents. *J. Med. Chem.* **2010**, *53*, 1347-1356.

(30) Cázares Marinero Jde, J.; Lapierre, M.; Cavaillès, V.; Saint-Fort, R.; Vessières, A.; Top, S.; Jaouen, G. Efficient new constructs against triple negative breast cancer cells: synthesis and preliminary biological study of ferrocifen-SAHA hybrids and related species. *Dalton Trans.* **2013**, *42*, 15489-15501.

(31) Wang, C. H.; Li, C. H.; Zhou, H. B.; Huang, J. High-throughput screening assays for estrogen receptor by using coumestrol, a natural fluorescence compound. *J. Biomol. Screen.* **2014**, *19*, 253-258.

(32) Anstead, G. M.; Carlson, K.; Katzenellenbogen, J. A. The estradiol pharmacophore: ligand structure-estrogen receptor binding affinity relationships and a model for the receptor binding site. *Steroids* **1997**, *62*, 268-303.

(33) Labrie, F.; Labrie, C.; Bélanger, A.; Simard, J. Third-and Fourth-Generation SERMs. In *Selective Estrogen Receptor Modulators*, Springer: 2002; pp 167-187.

(34) Gryder, B. E.; Rood, M. K.; Johnson, K. A.; Patil, V.; Raftery, E. D.; Yao, L. P.; Rice, M.; Azizi, B.; Doyle, D. F.; Oyelere, A. K. Histone deacetylase inhibitors equipped with estrogen receptor modulation activity. *J. Med. Chem.* **2013**, *56*, 5782-5796.

(35) Katzenellenbogen, J. A. The 2010 Philip S. Portoghese Medicinal Chemistry Lectureship: addressing the "core issue" in the design of estrogen receptor ligands. *J. Med. Chem.* **2011**, *54*, 5271-5282.

(36) Dadiboyena, S. Recent advances in the synthesis of raloxifene: a selective estrogen receptor modulator. *Eur. J. Med. Chem.* **2012**, *51*, 17-34.

(37) Maximov, P. Y.; Fernandes, D. J.; McDaniel, R. E.; Myers, C. B.; Curpan, R. F.;

Jordan, V. C. Influence of the length and positioning of the antiestrogenic side chain of endoxifen and 4-hydroxytamoxifen on gene activation and growth of estrogen receptor positive cancer cells. *J. Med. Chem.* **2014**, *57*, 4569-4583.

(38) Zheng, Y. F.; Zhu, M. H.; Srinivasan, S.; Nwachukwu, J. C.; Cavett, V.; Min, J.; Carlson, K. E.; Wang, P. C.; Dong, C.; Katzenellenbogen, J. A.; Katzenellenbogen, B. S.; Nettles, K. W.; Zhou, H. B. Development of selective estrogen receptor modulator (SERM)-like activity through an indirect mechanism of estrogen receptor antagonism: defining the binding mode of 7-oxabicyclo[2.2.1]hept-5-ene scaffold core ligands. *ChemMedChem* **2012**, *7*, 1094-1100.

(39) Shiau, A. K.; Barstad, D.; Loria, P. M.; Cheng, L.; Kushner, P. J.; Agard, D. A.; Greene, G. L. The structural basis of estrogen receptor/coactivator recognition and the antagonism of this interaction by tamoxifen. *Cell* **1998**, *95*, 927-937.

(40) Park, S. Y.; Jun, J. A.; Jeong, K. J.; Heo, H. J.; Sohn, J. S.; Lee, H. Y.; Park, C. G.; Kang, J. Histone deacetylases 1, 6 and 8 are critical for invasion in breast cancer. *Oncol. Rep.* **2011**, *25*, 1677-1681.

(41) Ring, A.; Dowsett, M. Mechanisms of tamoxifen resistance. *Endocr. Relat. Cancer* **2004**, *11*, 643-658.

(42) Speirs, V.; Malone, C.; Walton, D. C.; Kerin, M. J.; Atkin, S. L. Increased expression of estrogen receptor beta mRNA in tamoxifen-resistant breast cancer patients. *Cancer Res.* **1999**, *59*, 5421-5429.

(43) Pujol, J. L.; von Pawel, J.; Tumolo, S.; Martoni, A.; Hearn, S.; Fields, S. Z.; Ross, G. Preliminary results of combined therapy with topotecan and carboplatin in advanced non-small-cell lung cancer. *Oncology* **2001**, *61(Suppl 1)*, 47-54.

(44) Huey, R.; Morris, G. M.; Olson, A. J.; Goodsell, D. S. A semiempirical free energy force field with charge-based desolvation. *J. Comput. Chem.* **2007**, *28*, 1145-1152.

(45) Audie, J. Development and validation of an empirical free energy function for calculating protein-protein binding free energy surfaces. *Biophys. Chem.* **2009**, *139*, 84-91.

Table of Contents Graphic